Chemical Geology 580 (2021) 120381

Contents lists available at ScienceDirect

Chemical Geology

journal homepage: www.elsevier.com/locate/chemgeo

Invited Research Article

A decade of progress in understanding cycles of trace elements and their isotopes in the oceans☆

T.M. Conway [a,*], T.J. Horner [b], Y. Plancherel [c], A.G. González [d]

[a] College of Marine Science, University of South Florida, St Petersburg, FL, USA
[b] NIRVANA Labs, Woods Hole Oceanographic Institution, Woods Hole, MA, USA
[c] The Grantham Institute for Climate Change and the Environment, Earth Sciences and Engineering Department, Imperial College London, London, UK
[d] Instituto de Oceanografía y Cambio Global, IOCAG, Universidad de Las Palmas de Gran Canaria, ULPGC, Spain

ARTICLE INFO

Editor: Michael E. Boettcher

Keywords:
GEOTRACES
Southern Ocean
radionuclides
transition metals
marine geochemistry

ABSTRACT

We present an overview of a Virtual Special Issue (VSI) entitled "*Cycles of trace elements and isotopes in the ocean - GEOTRACES and beyond.*" In addition to hosting the overview of the GEOTRACES Intermediate Data Product 2017, we highlight the contents of 30 other articles that comprise the VSI. These articles contribute to the International GEOTRACES mission in four areas of discovery: developments in marine transition metal isotope analysis; the role of the Southern Ocean in driving global trace element cycling; advances in understanding of the utility of rare-earth elements and natural and anthropogenic radionuclides as tracers of ocean processes; and using aerosols, particles, and elemental speciation to interrogate processes driving trace element cycles. We close by highlighting the future direction of developments in the field.

1. Special issue overview

This Virtual Special Issue (VSI), *Cycles of trace elements and isotopes in the ocean - GEOTRACES and beyond…,* consists of 31 chemical oceanographic studies concerning the chemical and isotopic distributions of trace elements and their isotopes (TEIs) throughout the global oceans. This VSI was inspired by two sessions at the Goldschmidt Conference in Paris in Summer 2017: *Non-Conventional Stable Isotopes in the Ocean: Novel Applications, Technological Advances, and Future Applications* (10h) and *Cycles of Trace Elements and Isotopes in the Ocean: GEOTRACES and Beyond* (10i). The VSI showcases the current state-of-the-art of the distribution and biogeochemical cycling of several TEIs, ranging from well-studied elements (e.g., Fe; Moffett and German, 2020) to relatively novel tracers such as Pt (López-Sánchez et al., 2019).

Advances in this field in the last decade have been driven by improvements in field sampling, chemical purification, automation and/or rapid-throughput, and improved analytical capabilities. Many of these improvements were inspired or facilitated by the activities of the International GEOTRACES Program (Frank et al., 2003; Anderson and Henderson, 2005; SCOR Working Group, 2007; Anderson et al., 2014), which has the stated mission: "*to identify processes and quantify fluxes that control the distributions of key trace elements and isotopes in the ocean, and to establish the sensitivity of these distributions to changing environmental conditions*" (GEOTRACES Planning Group, 2006). Indeed, driven largely by field programs like GEOTRACES and CLIVAR, the prevalence of TEI data in the oceans has experienced a figurative explosion in the last decade, revolutionizing our understanding of the processes that influence the marine distributions and cycling of TEIs (e.g., Anderson et al., 2014; Anderson, 2020; Grand et al., 2014; Urban et al., 2020). As such, it is fitting that this editorial comes just over ten years after the official launch of the GEOTRACES section program at the Ocean Sciences Meeting in Portland in 2010.

At the time of writing, GEOTRACES has released two intermediate data products (Mawji et al., 2015; Schlitzer et al., 2018) with a third to be launched in 2021, and an electronic atlas of sections and 3D scenes (https://www.egeotraces.org/). Participating GEOTRACES countries have completed over 120 section, process study, or compliant cruises in all oceans as well as in several marginal basins (https://www.bodc.ac.uk/geotraces/cruises/programme/). Here, we provide an overview of the articles featured in this VSI, as well as highlighting the four wider fields of discovery that this collection touches upon. It is not, however, our intention to review the entire field of TEI research that GEOTRACES and

☆ This article and Virtual Special Issue are dedicated to Thomas M. Church, who was instrumental in driving forward our understanding of the coastal margins and atmosphere as boundary sources of TEIs to the oceans.

* Corresponding author.
E-mail address: tmconway@usf.edu (T.M. Conway).

https://doi.org/10.1016/j.chemgeo.2021.120381
Received 28 May 2021; Received in revised form 3 June 2021; Accepted 5 June 2021
Available online 8 June 2021

other field programs have facilitated in recent years. Instead, we point the reader to several recent review papers and collections that have grown out of GEOTRACES synthesis workshops and provide a more comprehensive overview of advances in our understanding of TEI cycling, boundary exchange, or paleoproxies in the oceans (e.g., Henderson, 2016; Hayes et al., 2018, 2021; Lam and Anderson, 2018; Anderson, 2020; Close et al., 2021; Horner et al., 2021).

2. Research highlights of this VSI

Below we provide a brief history of the GEOTRACES Program (Section 2.1) and introduce the 2017 Intermediate Data Product (Section 2.2), then we explore four areas of discovery featured in this VSI: developments in analytical methods for measurement of transition metal isotope systems in marine samples (Section 2.3), the role of the Southern Ocean in driving global TEI cycling (Section 2.4), advances in our understanding of ocean processes using rare-earth and radionuclide tracers (Section 2.5), and emerging insights into ocean TEI cycles from the study of aerosols, particles, and elemental speciation (Section 2.6).

2.1. History of the GEOTRACES program

The International GEOTRACES program, the first field program to present visualization of TEI distributions at high spatial resolution in the oceans, grew out of discussions at international conference sessions that culminated in an international planning workshop in Toulouse, France in 2003 (Frank et al., 2003). These endeavors ultimately led to the publication of a Science Plan in 2006 (GEOTRACES Planning Group, 2006) that continues to guide the GEOTRACES mission, science objectives, program structure, and timetable. A key objective of GEOTRACES is to standardize best practices for the collection and analysis of contamination-prone TEIs, to rigorously intercalibrate GEOTRACES and GEOTRACES-compliant datasets via a Standards and Intercalibration Committee, and to generate global data products (SCOR Working Group, 2007). Accordingly, the early years of the program (2008–2009) hosted two cruises (IC1 and IC2) in the North Atlantic and North Pacific oceans that acted as intercomparison exercises for many GEOTRACES TEIs prior to the start of the GEOTRACES field program in 2010 (Cutter and Bruland, 2012; Anderson et al., 2014). The outcome of these exercises was published in a special volume of L&O Methods (http://www.aslo.org/lomethods/si/intercal2012.html). These comprehensive activities to intercompare key GEOTRACES TEIs built on earlier inter-comparison efforts for a more limited set of TEIs that used 'SAFe' seawater reference standards, which were collected in the North Pacific in 2004 (Johnson et al., 2007). Although supplies of the SAFe standard materials are exhausted, these samples continue to be used as evidence for precision and accuracy by trace metal concentration analysts, supplemented by new seawater and dust standards (https://www.geotraces.org/standards-and-reference-materials/). Additionally, a GEOTRACES Methods Manual which provides best practices for TEI sampling and analysis was produced by the GEOTRACES Standards and Intercalibration Committee and is periodically updated and publicly available (Cutter et al., 2017).

The GEOTRACES field program officially began in 2010 with the first three Atlantic Section cruises (GA02; GA03; GA10; Anderson et al., 2014; Mawji et al., 2015), but the first GEOTRACES related cruises sailed in 2007-2008 as part of International Polar Year. By 2014, GEOTRACES launched their first publicly available 'Intermediate Data Product' (IDP2014), a global compilation of carefully inter-calibrated datasets from 15 cruises by 8 nations in the Arctic, Atlantic and Indian Oceans (Mawji et al., 2015). This product included discrete water data for numerous TEIs, together with CTD sensor data, and included 237 different parameters at 796 oceanic water column 'stations' (Mawji et al., 2015). This data was available through either direct download, or via an Electronic Atlas visualization of sections and 3D scenes (http://egeotraces.org; Mawji et al., 2015). The data product was also distributed to conference attendees in the form of USB keys. By launching data products during the lifetime of the program, it was hoped to strengthen community interactions, but also stimulate interest from other scientific communities (Mawji et al., 2015). The 2014 product also included data from several GEOTRACES-compliant cruises—expeditions that measured parameters of interest to the program but were not originally proposed as GEOTRACES sections. These expeditions are denoted by either the lowercase 'c' in cruise names (e.g., GAc01; Fig. 1), as GIPY for International Polar Year Cruises, or as GPpr for process studies.

2.2. The GEOTRACES Intermediate Data Product 2017

In 2017, GEOTRACES launched a second Intermediate Data Product (IDP2017), with a third planned for mid-2021 (IDP2021). In this VSI, we host the overview paper for the IDP2017 which summarizes the production of the product and its contents. Compared to the IDP2014, the IDP2017 represents an approximate doubling of oceanographic TEI data, with 46,794 samples from 810 stations from 39 cruises carried out by 11 countries between 2007 and 2014, and now covering the Arctic, Atlantic, Pacific, Southern and Indian Oceans (Fig. 1; Schlitzer et al., 2018).

Perhaps the most exciting addition to the 2017 Intermediate Data product is improved coverage of the vast Pacific Ocean, which was not covered by the 2014 Data Product. The Pacific data gap was important to close, since this basin played host to the first and most iconic trace metal profiles in the late 1970s (e.g., Boyle et al., 1976; Bruland et al., 1978), as well some of the first studies identifying that margin sediments were a potentially important ocean Fe source (Johnson et al., 1997). Since then, GEOTRACES section cruises in the Pacific have already led to paradigm shifts in understanding the importance of processes such as long distance transport of both sedimentary and hydrothermal Fe (Fig. 2; e.g., Fitzsimmons et al., 2014; Resing et al., 2015; Nishioka et al., 2020), and while the planned Atlantic GEOTRACES program is largely complete, section cruises in the Indian, Pacific, and Southern Oceans are likely to continue for at least another 5 years (Anderson et al., 2014). Lastly, the second GEOTRACES data product is the first to include aerosol and rain TEI data, as well as inclusion of GEOTRACES-compliant datasets.

The Indian Ocean is now the most-sparsely covered ocean, with only a single meridional GEOTRACES section (GI04) included in the GEOTRACES IDP 2017 (Fig. 1). However, despite the comparative paucity of GEOTRACES sections in the Indian Ocean, this VSI features several papers covering the region: Amakawa et al. (2019) feature the first Nd isotope ratios from the South West Indian Ocean, Barrett et al. (2018) present particulate data from CLIVAR sections in the Indian Ocean, Moffett and German (2020) features the distribution of Fe from GI04 in the Western Indian Ocean, and Wang et al. (2019a) present Ni and Zn isotope data from the Indian Sector of the Southern Ocean. Moffett & German also point in the direction of what will likely be a next phase of GEOTRACES—synthesizing and comparing multiple basin sections—in this case comparing Indian GI04 and Southeast Pacific GP16 Fe sections in order to advance understanding of globally relevant processes (Figs. 1–2). In this case, one of their findings is to highlight the importance of the so-called Fe shelf-basin 'shuttle' mechanism in moving dissolved Fe from the shelf to the deep ocean in multiple Oxygen Minimum Zones (Moffett and German, 2020), a mechanism that is also investigated in detail for the anoxic Black Sea in another article in this issue (Lenstra et al., 2019).

As detailed in Schlitzer et al. (2018), IDP submitting investigators had to proceed through rigorous data quality control, which required demonstration of data quality to the Standards and Intercalibration Committee via demonstrating suitability of sampling and analytical techniques as well as external comparability via measurement of SAFe standards, crossover stations (locations occupied by more than one GEOTRACES section cruise), or via similar approved methods. As such,

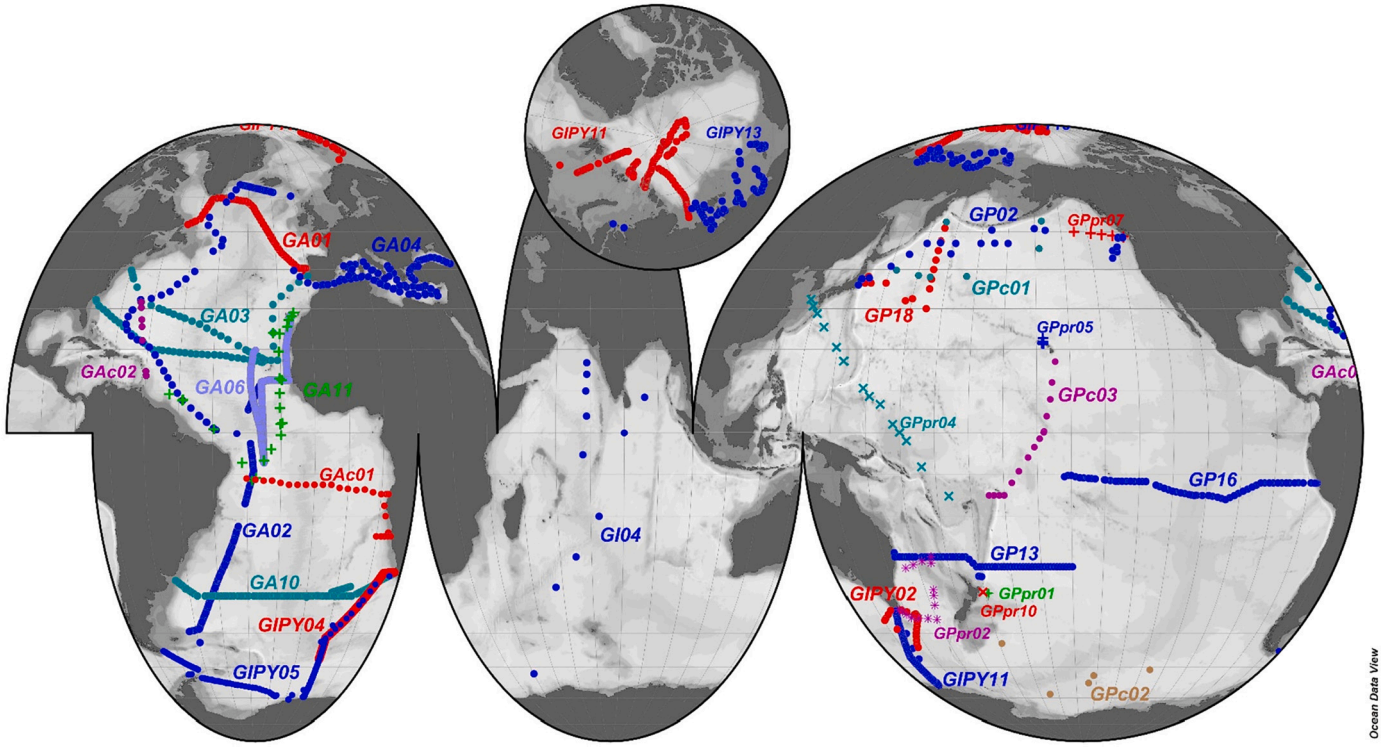

Fig. 1. Map showing GEOTRACES cruises included in the GEOTRACES Intermediate Data Product 2017. Figure reproduced from Schlitzer et al. (2018).

the data product can be viewed as an integrated product where datasets from different investigators and cruises can be compared. Use of crossover stations is vital for providing the opportunity to assess intercomparison of different cruises and laboratories for a suite of TEIs, but also provides the opportunity to assess potential temporal variability between cruises (e.g., Middag et al., 2015; Conway et al., 2016). Data included in the IDP2017 are available in three ways: downloading the entire dataset (https://www.bodc.ac.uk/geotraces/data/idp2017/); as customized data subsets (https://webodv.awi.de/login); or, through the GEOTRACES Electronic Atlas (http://www.egeotraces.org), which now includes 593 section plots (Figs. 1–2) and 132 animated scenes (Schlitzer et al., 2018). The customized subset option represents a significant advance in ease of access upon the first IDP, allowing data for single parameters or cruises to be more-easily downloaded. A continuously updated database of GEOTRACES and related field, modeling and laboratory-based publications on oceanic TEI cycling are also publicly available on the GEOTRACES website (https://www.geotraces.org/geotraces-publications-database/).

2.3. Developments in analysis of transition metal isotope systems in marine samples

Since 2006, a combination of improved metal-free laboratory practices and advances in multi-collector ICP-MS have facilitated measurement of the isotopic ratios of the bioactive transition metals (Cd, Cr, Cu, Fe, Ni, Zn) in seawater with the precision and accuracy required to resolve oceanic variability (i.e. <0.1‰). The first measurements of δ^{66}Zn and δ^{65}Cu in seawater were published in early 2006 (Bermin et al., 2006), closely followed by the first seawater data for δ^{114}Cd (though at the time, denoted $\varepsilon_{Cd/amu}$), which was published together with culture evidence that phytoplankton preferentially incorporate isotopically light Cd (Lacan et al., 2006). Evidence that phytoplankton exhibit a similar preference for light Zn in culture soon followed (John et al., 2007), as well as global evidence that biological uptake generatesdiscernable Cd isotope variations in the water column (Ripperger and Rehkämper, 2007; Ripperger et al., 2007). The first methods for analysis of δ^{56}Fe in coastal seawater were published in 2007 (de Jong et al., 2007), with the first method for measurement of open ocean δ^{56}Fe data presented by Lacan et al. (2008), requiring 10-20 L samples. This was then followed by further methods that refined the procedure and/or reduced the volume requirement to 1-4 L (John and Adkins, 2010; Lacan et al., 2010). By the onset of the GEOTRACES field program in 2010, however, published seawater measurements for δ^{56}Fe, δ^{65}Cu, δ^{66}Zn and δ^{114}Cd were limited to less than 60 per element, and no data for δ^{53}Cr and δ^{60}Ni (Table 1).

While early high-quality studies also showed the promise of these tracers (e.g., Vance et al., 2008; Abouchami et al., 2011; Radic et al., 2011; John et al., 2012), and early GEOTRACES intercomparison efforts broadly demonstrated the accuracy of different research groups (Boyle et al., 2012), it was the development of higher throughput, multi-elemental, techniques which facilitated the first application of these isotopes tracers to GEOTRACES ocean sections at high spatial resolution (e.g., Conway et al., 2013; Conway and John, 2014a). At the time of writing, multiple groups have applied these isotope tracers to different GEOTRACES sections, which has led to a dramatic increase in the number of trace metal isotope data available from the global oceans, increasing from <60 per element in 2010 to >1,500 for δ^{56}Fe, and >2,000 for δ^{66}Zn and δ^{114}Cd (Table 1; Schlitzer et al., 2018). Slower progress has been made for Ni and Cu (Table 1), though the first oceanic dissolved δ^{60}Ni data was published in 2014, and recent studies are significantly expanding the oceanic δ^{60}Ni dataset (e.g., Wang et al., 2019a; Archer et al., 2020; Yang et al., 2020). Dissolved δ^{53}Cr was the latest system to be widely applied in seawater, largely lagging due to the difficulty of dealing with Cr's complex redox chemistry in seawater; the first inter-basinal δ^{53}Cr study came only in 2015 (Scheiderich et al., 2015). Since then, progress has been rapid, with this issue hosting the first deep ocean full water column profile of dissolved δ^{53}Cr in the North Pacific (Moos and Boyle, 2019); this profile adds to the rapidly growing oceanic dataset (>300 data) from the Atlantic, North and South Pacific, the North Atlantic, and the Southern Ocean (e.g., Goring-Harford et al., 2018; Rickli et al., 2019; Janssen et al., 2020; Nasemann et al., 2020).

With the notable exception of Cr, the dramatic advances in coverage

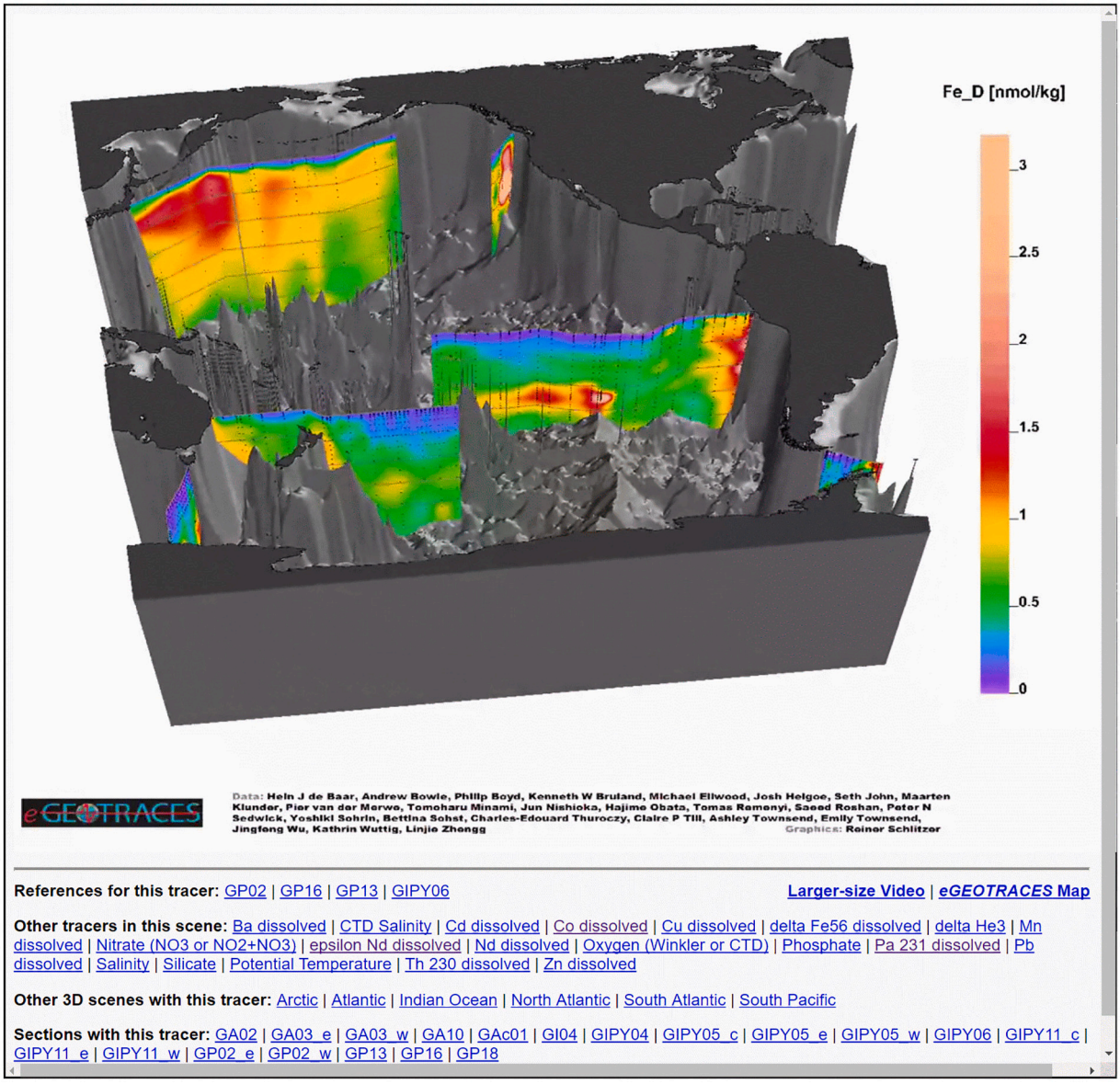

Fig. 2. An example three-dimensional scene available from the GEOTRACES electronic atlas (www.egeotraces.org/), showing dissolved Fe from multiple GEOTRACES cruises in the South Pacific. Figure reproduced from Schlitzer et al. (2018).

Table 1
Comparison of oceanic dissolved transition metal isotope data reported in 2010 compared to 2020, after 10 years of the GEOTRACES field program, ordered by data availability in 2010.

Isotope system	Published data in 2010	Published[b] data in 2020	Fold increase
$\delta^{114}Cd$[a]	53	2,683	>50
$\delta^{56}Fe$	37	1,718	>46
$\delta^{65}Cu$	32	434	>13
$\delta^{66}Zn$	14	2,023	>144
$\delta^{60}Ni$	0	274	-
$\delta^{53}Cr$	0	343	-

Data sources are shown at the end of the article.

[a] Note Cd isotope ratios are reported in the literature in several notations ($\varepsilon^{112}Cd$, $\varepsilon^{114}Cd$, $\varepsilon_{Cd/amu}$, or $\delta^{114}Cd$); here, we include all Cd isotope data as $\delta^{114}Cd$.

[b] Published also includes data included in the GEOTRACES IDP2017.

for most metal systems have been facilitated by the availability of low-blank, high-yield cation ion-exchange resins that bind multiple metals using nitrilotriacetic- or ethylenediaminetriacetic acid chelators, such as Nobias PA-1 (Hitachi; e.g., Sohrin et al., 2008) or Nitriloacetic Acid (NTA) Superflow resin (Qiagen; e.g., Lohan et al., 2005). Building on these earlier studies, these resins are now used in automated pre-concentration systems for metal concentration analysis (e.g., ESI seaFAST; Lagerström et al., 2013) and are also utilized by most groups to extract metals from seawater for stable isotope analysis (Lacan et al., 2008; John and Adkins, 2010; Takano et al., 2013; Conway et al., 2013; Rolison et al., 2018; Ellwood et al., 2020; Archer et al., 2020). Indeed, Nobias-PA1 resin is utilized by several studies in this issue for measurement of one or more of $\delta^{60}Ni$, $\delta^{65}Cu$, $\delta^{66}Zn$, and $\delta^{114}Cd$, including the first paired oceanic $\delta^{60}Ni$–$\delta^{66}Zn$ dataset, the first measurements of dissolved $\delta^{60}Ni$ in the Southern Ocean, and the first measurements of dissolved $\delta^{114}Cd$ in the Pacific sector of the Southern Ocean or $\delta^{65}Cu$ in the South Atlantic Ocean (Little et al., 2018; Sieber et al., 2019a; Wang et al., 2019a).

Despite initially lagging the other transition metals, the oceanic

δ^{65}Cu dataset, like δ^{53}Cr, is progressing at pace (Table 1); this is highlighted by two studies in this VSI which focus on δ^{65}Cu in the South Atlantic Ocean (Little et al., 2018) and Mediterranean Sea (Baconnais et al., 2019). Both papers highlight the emerging utility of δ^{65}Cu as a source and process tracer, adding to the growing consensus that the deep ocean δ^{65}Cu reservoir is relatively homogenous at near +0.7‰. Set against this background, however, Little et al. also find that the particulate δ^{65}Cu pool can be characterized into two pools (labile and refractory) that have distinct isotope signatures, similar to what has been observed in marine sediments. Little et al. also show that both benthic and estuarine inputs of Cu to the South Atlantic are associated with light dissolved δ^{65}Cu anomalies, suggesting that Cu isotopes may be a sensitive tracer of Cu source that is difficult to discriminate from concentration alone (Little et al., 2018). Similarly, and in agreement with previous work by Takano et al. (2014), Bacconais et al. show that both biological activity and Cu sources also leveraged distinct changes in dissolved δ^{65}Cu in Mediterranean surface waters, specifically via addition of light Cu from atmospheric dust, scavenging of light Cu associated with the euphotic zone, heavy Cu added by riverine outflow from mining and also light Cu associated with benthic inputs (Baconnais et al., 2019).

Possible use of δ^{65}Cu as a source tracer highlights the differential behavior of trace metals -and utility of trace metal isotopes- in the oceans, reflecting recent findings that benthic and atmospheric addition of Zn can be observed as light dissolved δ^{66}Zn anomalies in ocean sections (e.g., Conway and John, 2014b; Lemaitre et al., 2020a; Liao et al., 2020), but that the longer residence time of Cd or Ni in the oceans means that these isotope systems do not generally show anomalies linked to sources. Indeed, Xie et al. (2019a) demonstrate that there is little observable external influence on [Cd] and δ^{114}Cd from riverine and natural dust sources to the North Atlantic, with δ^{114}Cd instead being dominated by biological cycling and ocean circulation. Unlike measurements of Cd and Zn isotopes, however, key questions remain about the fidelity of different analytical techniques for measurement of both [Cu] and δ^{65}Cu, especially about the role of acidification strength, UV oxidation, and storage time prior to analysis (Posacka et al., 2017; Little et al., 2018; Baconnais et al., 2019). Both Cu studies in this VSI note that [Cu] is systematically higher in seawater samples that are UV oxidized prior to analysis, and that although most reported deep ocean δ^{65}Cu values range from +0.6 to +0.7‰, there is disagreement by up to 0.2‰ on consensus standards (Little et al., 2018; Baconnais et al., 2019). Such observations highlight the challenges of measuring trace metal isotope ratios in seawater, especially for elements that are strongly complexed by organic ligands and for which double-spiking, which requires four stable isotopes, is not possible. As δ^{65}Cu continues to be applied as an oceanic tracer, we repeat the call of Little et al. (2018) that both a robust Cu isotope intercalibration exercise and the establishment of best practices are urgently needed.

Several papers in this issue also revisit the fractionation of stable isotopes during biological uptake by phytoplankton (e.g., Köbberich and Vance, 2019; Wang et al., 2019a). Despite being part of the earliest marine trace metal isotope research (Lacan et al., 2006), and the widespread observations that biological uptake and regeneration appears to shape the isotopic distributions of several of the trace metals (reviewed in detail in Horner et al., 2021), this is an area of the field that arguably lags the GEOTRACES-driven explosion of field data. Indeed, understanding the isotope fractionation factors associated with different species remains poorly constrained for all the trace metals. Köbberich and Vance (2019) address this paucity of species data for δ^{66}Zn, presenting the first culture data for Zn incorporation by cyanobacteria and comparison with several species of diatoms as well as the literature (see Fig. 3). Their study confirms previous findings that uptake of Zn into cells occurs with an almost-universal preference for light isotopes in culture (e.g., John et al., 2007; John and Conway, 2014; Samanta et al., 2018), but also warns that some of this 'apparent' fractionation observed in culture may be the result of using an organic chelator such as EDTA (Köbberich and Vance, 2018). The authors postulate that this overestimation of uptake fractionation in culture may explain why such muted δ^{66}Zn variability is seen in Southern Ocean water column data in comparison to systems such as δ^{114}Cd (e.g., data presented by Sieber et al., 2019a and Wang et al., 2019a).

Further potential complexity for interpreting oceanic surface δ^{66}Zn patterns arises from possible uptake of heavy Zn by diatoms in culture under Fe-limitation or scavenging of Zn to organic matter (John and Conway, 2014; Köbberich and Vance, 2017; Weber et al., 2018), although such effects do not appear to be obvious from the first Southern Ocean studies of δ^{66}Zn under various states of Fe limitation (Wang et al.,

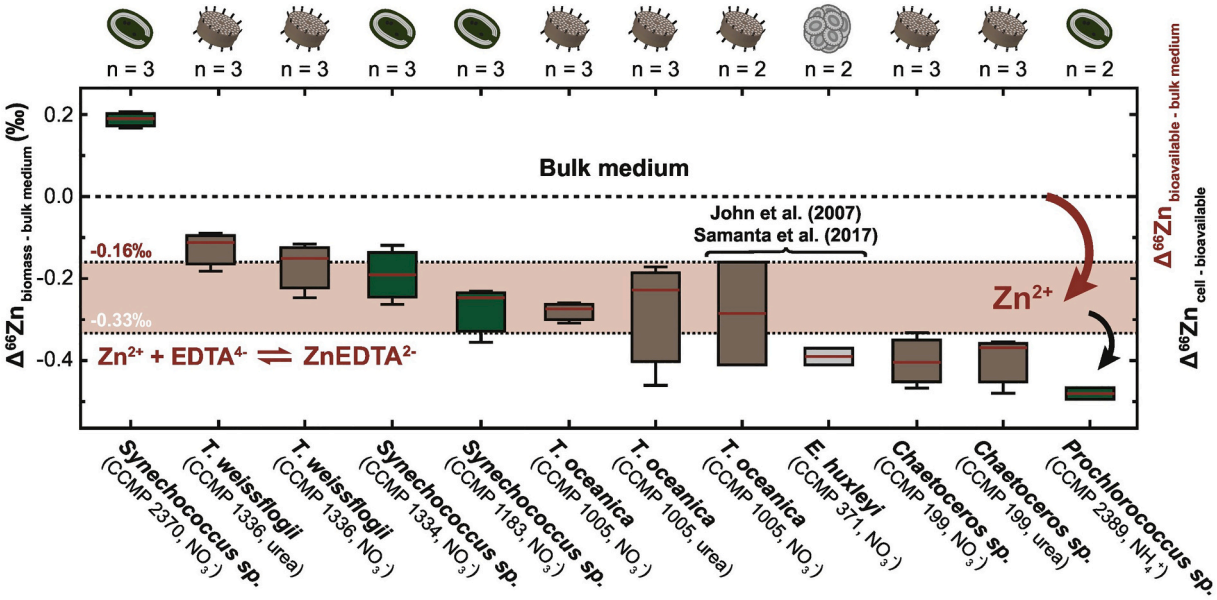

Fig. 3. A summary of culture studies on the fractionation of Zn isotopes during uptake by marine phytoplankton. Boxes show measured biomass δ^{66}Zn composition relative to the media for cyanobacteria (*Synechococcus* sp., *Prochlorococcus sp.*), diatoms (*T. weissflogii, T. oceanica, Chaetoceras* sp.), and coccoliths (*E. huxleyi*). The orange bar denotes the expected signature of bioavailable Zn when culturing with the chelator EDTA. Figure reproduced with permission from Köbberich and Vance (2019).

2019a; Sieber et al., 2020). As such, while such advances in our understanding of δ^{66}Zn fractionation in culture do highlight the intriguing value that trace metal isotope measurements bring to understanding trace metal biogeochemistry, they demonstrate that more marine process studies are needed. For other systems, such as δ^{56}Fe and δ^{60}Ni, there is some mixed evidence for fractionation in field data (e.g., Wang et al., 2019a; Archer et al., 2020; Yang et al., 2020; Ellwood et al., 2015; Ellwood et al., 2020), but there is currently a lack of culture studies of uptake fractionation for these elements.

2.4. The role of the Southern Ocean in driving global TEI cycling

Early trace element concentration datasets, which observed tight global correlations between elements such as Cd and phosphate, or Zn and silicate, were primarily interpreted in terms of one-dimensional vertical profiles, dominated by the processes of biological uptake, regeneration, and scavenging (e.g., Boyle et al., 1976; Bruland, 1980; de Baar et al., 1994). These processes were invoked to explain low concentrations of TEIs such as Cd and Zn in surface waters, along with enrichment into deep waters by dissolving biogenic material along the oceanic 'conveyor'. Similarly, dissolved Fe profiles were largely considered as a balance of surface addition, uptake, regeneration, and scavenging (see Boyd and Ellwood, 2010). By the early 2000s, however, focus had switched to the dominant role of the Southern Ocean 'hub' in driving the low latitude distributions of the macronutrients nitrate, phosphate, and silicate (e.g., Sarmiento et al., 2004; Marinov et al., 2006). This view holds that a combination of upwelling of nutrient-rich deepwater and surface processes of uptake and regeneration within the Antarctic Circumpolar Current (ACC) of the Southern Ocean act to impart pre-formed nutrient signatures to subducting water masses which are then transported to the lower latitudes via ocean circulation. As such, at first order, the differing oceanic profiles of macronutrients such as P and Si arise not from the differing *in situ* length scales of 1D regeneration of these elements, but rather from supply of P and Si to intermediate depths by Southern-sourced water masses with differing P:Si preformed ratios (Sarmiento et al., 2004), with only a secondary role for addition of nutrients as water masses circulate (Sarmiento et al., 2007).

While early trace element studies recognized the role of Southern Ocean processes and ocean circulation in driving the low-latitude distribution of many TEIs (e.g., Broecker and Peng, 1982; Frew and Hunter, 1992), the extreme paucity of field data for the contamination prone TEI micronutrients in high latitude water-mass formation regions meant that by default a number of TEIs continued to be interpreted in largely 1D terms well into the GEOTRACES era, often dependent on sampling resolution. However, with the onset of the GEOTRACES program and release of Intermediate Data Products, much larger, more-accurate datasets for TEIs became available (Mawji et al., 2015; Schlitzer et al., 2018), facilitating a more 3D view of global cycling for many TEIs (e.g., http://www.egeotraces.org). For example, based on such datasets, recent studies have confirmed that the Southern Ocean and global water mass mixing are just as influential in driving the global distributions of Cd and Zn (and their correlations with macronutrients), as they are in driving the distributions of the macronutrients themselves (e.g., Baars et al., 2014; Abouchami et al., 2014; Vance et al., 2017; Middag et al., 2018).

Several studies now show that uptake of certain nutrients such as Si and Zn within the sub-Antarctic Zone of the ACC can lead to low preformed quantities of these nutrients in north-flowing waters that act as precursors for intermediate and mode waters (e.g., Sarmiento et al., 2004; Vance et al., 2017). Similarly, a combination of surface Southern Ocean processes and circulation have been invoked to explain the 3D distribution of isotope systems such as Cd, Si or Ba within the Atlantic Ocean (de Souza et al., 2012a; Abouchami et al., 2014; Horner et al., 2015), or Si in the Pacific (de Souza et al., 2012b). Preferential biological uptake of light Cd in Southern Ocean waters imparts a distinctly isotopically heavy δ^{114}Cd signature to intermediate water masses (+0.4 to +0.6‰) relative to the deep ocean (+0.2‰), with the presence of these southern-sourced water masses dominating the 1D vertical distribution of δ^{114}Cd well into the North Atlantic (e.g., Xue et al., 2012; Abouchami et al., 2014; Conway and John, 2015a).

Several articles in this issue add clarity to the view that Southern Ocean processes are important for understanding the distribution of TEIs, with Sieber et al. (2019a) presenting the first meridional dataset of dissolved Cd and δ^{114}Cd in the South Pacific Ocean from Japanese GEOTRACES Section GP19. This work further highlights the importance of Southern Ocean surface processes in setting preformed Cd:P and isotopically heavy δ^{114}Cd to AAIW and AASW, which then advect northward with δ^{114}Cd signatures conserved into the low-latitude Pacific Ocean (Sieber et al., 2019a). The presence of elevated δ^{114}Cd in intermediate water masses influencing the low-latitude intermediate depth Pacific Ocean can be seen in Fig. 4, analogous to that demonstrated previously for δ^{114}Cd in the Atlantic Ocean (Abouchami et al., 2014) and for δ^{30}Si in the South Pacific (de Souza et al., 2012b). In contrast, the muted δ^{66}Zn fractionation during uptake in the Southern Ocean shown by Wang et al. (2019a), when combined with more recent research by Sieber et al. (2020), demonstrate that uptake of Zn in the Southern Ocean cannot exert an equivalent influence on the low-latitude distribution of dissolved δ^{66}Zn.

Outside of the Antarctic, Sieber et al. (2019a) find that almost all variability in δ^{114}Cd and Cd along the GP19 section can be attributed to the effects of transport and mixing of preformed signals, with only small roles for remineralization; this finding is also consistent with what has been reported for dissolved Cd in the Atlantic (Xie et al., 2015; Middag et al., 2018). In this VSI, Xie et al. (2019a) present new data from the tropical Atlantic Ocean, which also supports the dominance of water-mass mixing on driving Cd:P and δ^{114}Cd throughout the Atlantic Ocean. However, this study also highlights the complexity in low-latitude Cd cycling that can be caused by processes that appear to decouple Cd from P *in situ*, such as addition of Cd, preferential regeneration of either Cd or P in sinking organic matter, or loss of Cd to particulates in sulfides in oxygen minimum waters, that has been proposed by Janssen et al. (2014) previously in both the North Atlantic and North Pacific Oceans (Xie et al., 2019a).

Despite the importance of Southern Ocean surface processes in ultimately setting the pre-formed concentrations of different water masses that advect northward, Southern Ocean TEI studies are often restricted to Austral Summer for obvious logistical reasons. However, since deep winter mixing and entrainment have been shown to play an important role in both supplying metals to sustaining summer productivity, 'resetting' the system, and playing a role in TEI cycling in the Southern Ocean (e.g., Tagliabue et al., 2014; Sieber et al., 2020), our understanding of TEI cycling processes occurring in winter remains an important knowledge gap. Beginning to address that paucity of data, in this issue Cloete et al. (2019) present TEI data ([Cu], [Ni] and [Zn]) from expeditions in the Atlantic Sector of the Southern Ocean over a full austral-winter cycle. Their findings include insights into winter TEI cycling, specifically that [Cd], [Zn] and [Ni] are higher in mixed layers in winter compared to summer, attributed to lower productivity and differential incorporation of metals relative to macronutrients under low-light levels in austral winter. The latter finding adds weight to studies suggesting that deeper winter mixing might impart distinctive metal:nutrient ratios and/or trace metal isotopic signatures that are preserved in remnant winter water during summer and highlights both a need for more seasonal-resolution data in the Southern Ocean, and more data coverage from high latitude water-mass formation regions in general.

2.5. Advances in understanding of the utility of rare-earth elements and natural and anthropogenic radionuclides as tracers of ocean processes

Similar to the bioactive trace metals and their isotopes, the onset of

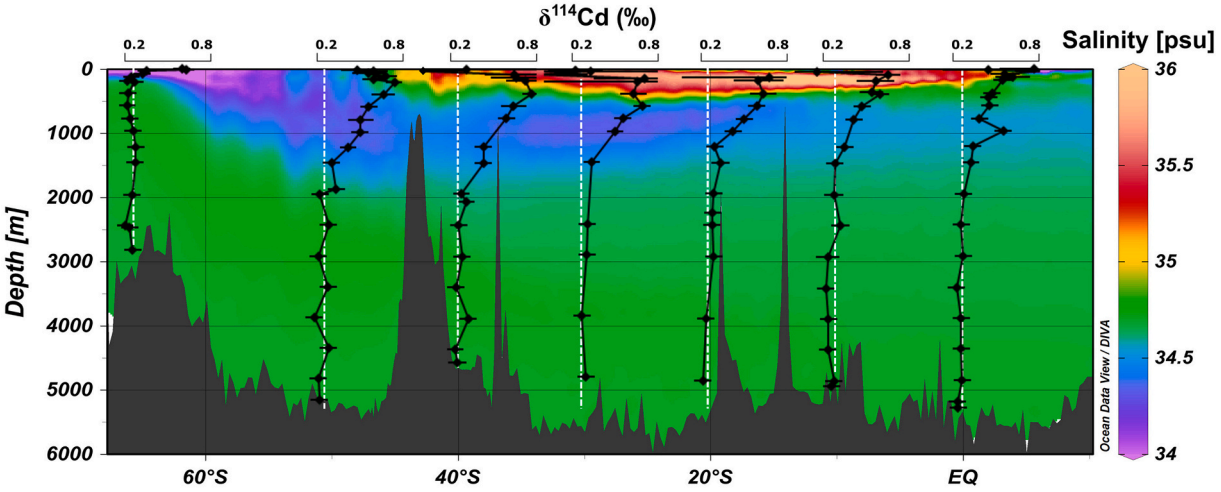

Fig. 4. Dissolved cadmium isotope ratios (δ^{114}Cd) from GEOTRACES GP19 transect along longitude 170°W in the Southwest Pacific Ocean. This figure shows how surface processes in the Southern Ocean can impart a preformed signature to intermediate depths at low latitudes, with the northward proliferation of Antarctic Intermediate Water visible in low salinity and elevated δ^{114}Cd. Figure reproduced with permission from Sieber et al. (2019a).

large field programs such as GEOTRACES has spurred on analytical development of methods to measure and field application of a range of natural and anthropogenic radionuclides (e.g., He, Ra, Th, U, Pu), rare earth elements (Nd, Hf etc.), and radiogenic isotope systems (e.g., ^{143}Nd/^{144}Nd) throughout the oceans. Indeed, dissolved measurements of the radiogenic ^{143}Nd/^{144}Nd ratio (typically expressed as εNd) are classified as a GEOTRACES required 'key parameter', meaning that εNd should, in principle, be measured on all GEOTRACES cruises (GEOTRACES Planning Group, 2006). Here we feature some of the contributions from articles in this VSI to advancing the use of both naturally occurring (εNd, Ra) and anthropogenic radionuclides as tracers (^{236}U, ^{239}Pu/^{240}Pu).

2.5.1. Neodymium

The utility of the radiogenic εNd ratio in the ocean arises because water masses acquire distinct εNd based on where they acquired their Nd. Neodymium is added to seawater by weathering of continental rocks, which exhibit considerable spatial variability in ^{143}Nd/^{144}Nd depending on age and composition (see recent compilation by Robinson et al., 2021). Moreover, the residence time of dissolved Nd is shorter than the oceanic mixing time, meaning that seawater is spatially variable for εNd (e.g., Frank, 2002; Jeandel et al., 2007). Although εNd were first measured in seawater and identified as a potential water mass tracer by pioneering studies such as Piepgras et al. (1979), applied as paleoproxies for water mass circulation in archives such as ferromanganese crusts as early as the 1980s (e.g., Goldstein and O'Nions, 1981; Albarède and Goldstein, 1992), and a large global database of seawater εNd available by 2011 (see Lacan et al., 2012 and references therein), it was not until the onset of the GEOTRACES era that widespread dissolved εNd section datasets have become available. Indeed, the number of dissolved εNd measurements made between 2011 and 2016 exceeded the total measured in the last 30 years (reviewed by van de Flierdt et al., 2016), with the GEOTRACES IDP 2017 featuring nine ocean sections (Schlitzer et al., 2018). GEOTRACES also facilitated interlaboratory intercomparison exercises for groups measuring εNd in seawater and marine particles (van de Flierdt et al., 2012; Pahnke et al., 2012). Reflecting the findings of earlier studies, the first GEOTRACES εNd sections in the Atlantic (GA02 and GA03; Stichel et al., 2015; Lambelet et al., 2016) largely confirmed the utility of εNd as a water mass tracer, further constraining the εNd endmember signature of North Atlantic Deep Water masses in detail (van de Flierdt et al., 2016). However, such studies also provided evidence for the variable importance of local boundary exchange in modifying dissolved εNd but not [Nd] (e.g., Lacan and Jeandel, 2005; Jeandel, 2016), as well as further evidence that internal cycling such as reversible scavenging of Nd to biogenic particles acts to decouple Nd and εNd distributions (e.g., Siddall et al., 2008; Stichel et al., 2020).

In this issue, several studies provide further insight into the processes controlling both the marine cycling of [Nd] and the utility of εNd as a water mass tracer. Morrison et al. and Laukert et al. present new high-resolution datasets from the high-latitude North Atlantic, namely around Iceland and the Barents Sea respectively, while Amakwara et al. present the first εNd from the South West Indian Ocean and Zieringer et al. present new data from the tropical eastern Atlantic (Amakawa et al., 2019; Laukert et al., 2019; Morrison et al., 2019, Zieringer et al., 2019). These articles highlight the dominance of conservative mixing of water masses (with distinct εNd) in controlling εNd distributions in the ocean, and place better constraints on the endmember εNd signature of water masses in their respective areas of study. The studies also examine the influence of local processes which could compromise the use of regional εNd as a circulation tracer. For example Morrison et al. (2019) investigate the possibility of addition of uniquely-radiogenic εNd from weathering of basalts on Iceland, but find that such an addition of [Nd] only affects the εNd of local coastal waters, rather than compromising the εNd signature of other major water masses in the Iceland Basin. In contrast, Zieringer et al. (2019) show that, similar to previous work by Stichel et al. (2015) and Rickli et al. (2010), surface waters of the tropical eastern Atlantic are significantly impacted by seasonally- and spatially-variable deposition of Saharan dust, manifesting in both [Nd] and εNd, potentially weakening the use of εNd as a water mass tracer in this region. Zieringer et al. also confirm the importance of boundary exchange associated with Canary Island and Cape Verde volcanism for modifying εNd throughout the whole water column in this region while not changing [Nd], as shown previously by Rickli et al. (2010). Also in this issue, Pham et al. (2019) investigate [REE] distributions in the Solomon Sea and show that this region exports elevated Nd at intermediate depths into the equatorial Pacific undercurrent from continental weathering, but also find that no elevated Nd is seen in surface waters. Lastly all three εNd studies demonstrate the removal of Nd by scavenging to particles without a noticeable change in εNd, providing further weight to the widespread importance of this process for decoupling [Nd] and εNd in the oceans (Laukert et al., 2019; Morrison et al., 2019; Zieringer et al., 2019; Stichel et al., 2020).

2.5.2. Radium

The four common naturally-occurring radionuclides of Ra (^{223}Ra,

^{224}Ra, ^{226}Ra, ^{228}Ra) are present in trace quantities in the ocean forming from the decay of their parent Th isotopes in sediments. Radium is soluble in seawater and so Ra produced in sediments diffuses out of sediment pore waters into the water column where the different Ra isotopes behave 'essentially conservatively', but with half-lives ranging from 3 days to 1,600 years (e.g., Charette et al., 2015). As such, the longer-lived Ra isotopes (^{226}Ra, 1,600 yr; ^{228}Ra 6 yr) have been long been applied as tracers for calculating fluxes to the coastal environment from processes such as riverine addition or submarine groundwater discharge (SGD), both at the local and basin scale (e.g., Moore, 1969; Moore and Shaw, 2008). The shorter-lived isotopes (^{223}Ra, 11 d; ^{224}Ra, 4 d) are increasingly used to determine coastal mixing rates (e.g., Moore, 2000), providing rate information for understanding processes that cycle TEIs. With the development of new methods for high-throughput processing of marine samples for all four Ra isotopes, intercomparison efforts, and the onset of the GEOTRACES program, Ra isotope distribution datasets have undergone a similar increase in data to that of the other TEIs (e.g., Charette et al., 2012; Henderson et al., 2013; Schlitzer et al., 2018). This increase in data has facilitated a more detailed examination of the role of different boundary processes in influencing oceanic distribution of all four Ra radioisotopes, as well as being useful for constraining fluxes from these boundaries and calculating water mass ages (e.g., Charette et al., 2015; Sanial et al., 2018; Kipp et al., 2019; Garcia-Orellana et al., 2021).

Further, GEOTRACES synthesis efforts have made use of global modelling and ^{228}Ra datasets to use Submarine Groundwater Discharge (SGD) ^{228}Ra fluxes to quantify SGD fluxes of other TEIs to the oceans (e.g., Kwon et al., 2014; Charette et al., 2016; Mayfield et al., 2021). A similar approach is made by Roy-Barman et al. (2019) in this issue, where they use ^{228}Ra to constrain SGD Ba fluxes to the Mediterranean Sea as part of the GA-04S MedSeA GEOTRACES cruise and show that such fluxes can be significant to the dissolved Ba budget. Also in this issue, Neuholz et al. (2020) highlight a second use of the short lived ^{224}Ra and ^{223}Ra isotopes, using them above the Brothers Volcano hydrothermal system on the Kermedec Arc to determine hydrothermal plume age, and calculate the relative roles of eddy diffusion and advection for plume dispersion. This study is the first to look at an interarc volcanic system, showing that diffuse flow takes five days longer to reach the plume than direct venting (Neuholz et al., 2020), and builds on previous studies using both short- and long-lived Ra isotopes to quantify fluxes, plume ages and dispersion at hydrothermal sites such as Puna Ridge, the Mid Atlantic Ridge TAG vent site, and the East Pacific Rise (Moore et al., 2008; Kipp et al., 2018).

2.5.3. *Artificial radionuclides*

Since the onset of the nuclear age, there has been substantial public concern about the environmental and health impacts of the release of radioactive nuclides into the natural environment. These anthropogenic-derived radionuclides are principally released as fallout from atom bomb testing (typically released to the atmosphere), or from nuclear reactor accidents (can be atmospheric or oceanic release). While a concern for environmental health, such accidental releases have also led to serendipitous opportunities to use measurements of some of these anthropogenic radionuclides to trace ocean processes, also stimulated by the GEOTRACES program. For example, in this issue Villa-Alfagme et al. present the first measurements of the long-lived radioisotope ^{236}U from GP16 cruise in the Eastern Tropical Pacific by AMS (Villa-Alfageme et al., 2019). They show that concentrations reach as low as 1000 atoms kg^{-1} in the deep Pacific, and that ^{236}U, when combined with other tracers such as Δ14C and ^{3}He, can be useful for constraining water mass mixing in the region (Villa-Alfageme et al., 2019). Secondly, Wu et al. (2019) present measurements of $^{240/239}$Pu in samples collected in 2014-2015 from the Kuroshio Current near Japan, to assess the regional impact of radioactive release of Pu from the Fukushima Daiichi Nuclear Power Plant Disaster in 2011. Their findings (reproduced in Fig. 5), show no impact of the accident on surface water ^{240}Pu/^{239}Pu in the wider region, but highlight the continuing influence of radioactive pollution from US nuclear testing in the Pacific Proving Grounds in combining with global nuclear fallout to set the $^{240/239}$Pu signature of North Pacific waters (Wu et al., 2019).

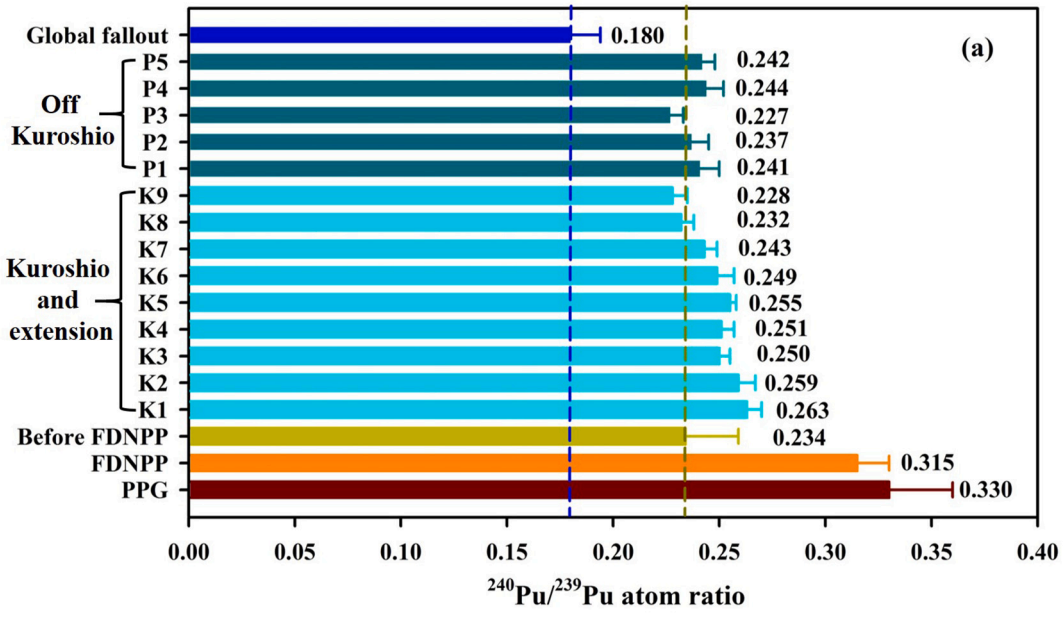

Fig. 5. Measurement of the dissolved anthropogenic radioactive contaminant plutonium (^{240}Pu/^{239}Pu) in the Kuroshio current and extension waters close to Japan (2014-2015) following the Fukushima Daiichi Nuclear Power Plant Disaster (FDNPP) in 2011. Figure compares seawater data with possible sources (global fallout, Pacific Proving Ground nuclear tests [PPG] and FDNPP), showing little impact of the Fukushima release on seawater ^{240}Pu/^{239}Pu. Figure reproduced with permission from Wu et al. (2019).

2.6. Aerosols, particles, and elemental speciation

2.6.1. Aerosols

As with seawater dissolved TEI measurements, collection of atmospheric dust has a long history, and the importance of atmospheric deposition to the marine Fe cycle has long been known, significantly predating large field programs like GEOTRACES (e.g., Duce et al., 1991; Duce and Tindale, 1991; Jickells et al., 2005). More recently, shipboard aerosol collection has facilitated characterization of soluble Fe and Al, and other TEIs in aerosols at greater resolution over the open ocean (e.g., Baker et al., 2006; Buck et al., 2006), adding to multiple decades of time series measurements from sites such as Barbados and Bermuda (e.g., Arimoto et al., 1995; Prospero et al., 2014). With the onset of cruises as part of large field programs like GEOTRACES, CLIVAR, and AMT (the Atlantic Meridional Transect), has come the further opportunity to couple atmospheric and surface ocean TEI measurements in order to dramatically increase coverage, understanding and synthesis of total and soluble TEI deposition fluxes to the global oceans (e.g., Buck et al., 2010, 2013; Grand et al., 2014; Shelley et al., 2015; Shelley et al., 2017; Jickells et al., 2016; Barraqueta et al., 2019). Coupling of elements such as ^{7}Be or ^{230}Th and ^{232}Th with aerosol TEIs has also led to improved flux estimates of dust and TEIs to the surface oceans (reviewed by Anderson et al., 2016).

This VSI contains two GEOTRACES aerosol 'sections', with Marsay et al. (2018) presenting the first high resolution TEI aerosol study from the western Arctic Ocean from GN01 in 2015, and Buck et al. (2019) examining aerosol fluxes to the Southeastern Tropical Pacific Ocean from GP16 in 2013. Measurements of aerosol TEI deposition fluxes are scarce in the climate-sensitive Arctic Ocean, and so it is significant that Marsay et al. provide a large aerosol TEI composition and solubility dataset to test and inform deposition models, as well as using ^{7}Be deposition to calculate TEI deposition fluxes; they show that summertime deposition fluxes of both mineral dust and Fe are low, typical of open marine air, yet the region does experience significant aerosol TEI contributions from anthropogenic pollution. In the tropical Southeastern Pacific, Buck et al. show a pronounced offshore negative gradient in both dust and Fe deposition moving offshore from Peru into open marine air, with elements such as Fe and Al coming from natural sources and other TEIs such as Cu, Cd, and Pb coming from anthropogenic sources (Buck et al., 2019). Buck et al. highlight the importance of atmospheric-derived Fe is greatly increased in the Fe-limited offshore portion of GP16, far from the Peruvian margin (Buck et al., 2019). Also in this issue, Chien et al. (2019) provide a time series analysis of TEI deposition to Lake Tahoe in California; like both open-ocean aerosol studies, they find a largely natural source of elements such as Fe, but an anthropogenic source of elements such as Pb or Cd.

2.6.2. Particles

Marine particles play a vital role in oceanic TEI cycling, acting as surfaces for permanent or reversible exchange with the dissolved phase, and thus act as both important sources and eventual sinks for dissolved TEIs (e.g., McDonnell et al., 2015; Jeandel et al., 2015). As reviewed by Jeandel et al. (2015), although oceanic programs such as JGOFS and GEOSECS provided a wealth of early understanding of the distribution and biogeochemistry of marine particles, the methods for collection and analytical tools to study most contamination-prone particulate trace elements were not available, highly limiting data coverage. With the onset of the GEOTRACES program however, efforts to review, refine, and intercalibrate clean large volume particulate sampling methods (e.g., McLane, MULVFS or SAPS pumps vs go-flo filtration), filter type, digest methods, and analytical tools such as optical, ICP-MS, X-ray and synchrotron techniques have led to vast leap forwards in our knowledge of single-particle and particle assemblage TEI chemistry (e.g., Bishop et al., 2012; McDonnell et al., 2015; Lam et al., 2015a; Boss et al., 2015). Accordingly, the GEOTRACES program has led to the first high-resolution ocean sections of TEIs such as Fe and Mn coupled to particle composition (i.e., lithogenic, authigenic, suspended organic matter, opal, carbonate; as well as a suite of minor TEIs and their isotopes (e.g., Lam et al., 2015b; Ohnemus and Lam, 2015; Lam et al., 2018; Hayes et al., 2015; Revels et al., 2015; Little et al., 2018; Gourain et al., 2019; Lemaitre et al., 2020b).

Two papers in this issue touch on the topic of particulate Ba cycling (Roy-Barman et al., 2019; Martinez-Ruiz et al., 2019). Marine particles play an integral role in the marine Ba cycle, with dissolved Ba removed from seawater by the precipitation of particulate barite during the microbial oxidation of sinking organic matter (e.g., Chow and Goldberg, 1960; Dehairs et al., 1980). The balance between barite precipitation and dissolution varies with depth, often leading to the development of significant particulate Ba standing stocks in the mesopelagic ocean (e.g., Lam et al., 2015b). However, questions remain about the exact mechanisms of barite precipitation in seawater, which is generally undersaturated with respect to barite (e.g., Church and Wolgemuth, 1972). Most studies agree that overcoming this thermodynamic barrier requires some form of biological mediation, and frequently invoke a microenvironment-mediated model of precipitation (e.g., Chow and Goldberg, 1960). Martinez-Ruiz et al. provide further insight into this process, using mineralogical and crystallographic analyses of size-fractionated marine particles to suggest that pelagic barite forms in two steps: first as an amorphous Ba phosphate-rich phase in association with extracellular polymeric substances that is later substituted by sulfate to form barite. These observations are consistent with other recent findings pointing toward the importance of organic matter—and specifically biofilms—in mediating barite precipitation in undersaturated waters (e.g., Horner et al., 2017; Deng et al., 2019; Martinez-Ruiz et al., 2020). However, the second Ba study in this VSI, by Roy-Barman et al., finds that organic matter regeneration may contribute to the dissolution of particulate barite in the Mediterranean Sea, highlighting additional complexity in the marine geochemical cycle of Ba.

This VSI also hosts several papers which focus on particle cycling and the interaction of dissolved and particulate phases in the ocean, especially highlighting the contribution of other field programs such as CLIVAR and the Bermuda Atlantic Time Series (Barrett et al., 2018; Conte et al., 2019). Barrett et al. (2018) present a transect of trace elements in suspended particulate matter (Al, Si, P, Ca, Fe and Zn) from three US CLIVAR/CO_2 repeat hydrography sections (I09N/I08S/I06S) in the Indian and Southern Oceans, stretching from either India or South Africa to Antarctica. This work, which adds a wealth of particulate TEI data to a particularly poorly sampled region, highlights the unexpected importance of biogenic $CaCO_3$ in scavenging dissolved Al to particles in regions of high productivity, examines particulate Al and Fe sources across the region, and documents the elevated uptake of Zn by Southern Ocean diatoms with elevated Zn:P ratios (Barrett et al., 2018). The latter finding confirms the importance of high Southern Ocean Zn and Si uptake by Fe-limited diatoms in influencing the global distribution of Zn relative to Si (Twining and Baines, 2013; Vance et al., 2017). Conte et al. (2019) examine the composition and TEI content of particles reaching the deep Sargasso Sea in the North Atlantic, making use of a 15-year time series at the BATS site (Fig. 6.). Their findings highlight the importance of understanding seasonality for understanding particle type, particle-TEI exchange (e.g., biogenic fluxes of TEIs and/or scavenging of TEIs to authigenic Mn oxides), as well as the role of margin sediments in supplying lithogenic particles to the deep Atlantic (Conte et al., 2019). Lastly, Cheize et al. (2019) provide an elegant particle incubation experiment that shows that resuspension of benthic particles is a large source of Fe and Mn, but that release of these elements is decoupled in time and by particle type. Such time-series datasets and small-scale process studies provide invaluable insights into seasonal to inter-annual variability, which are essential for placing the findings of 'snapshot' GEOTRACES datasets in context.

2.6.3. Elemental speciation

Alongside the GEOTRACES-facilitated data explosion in dissolved

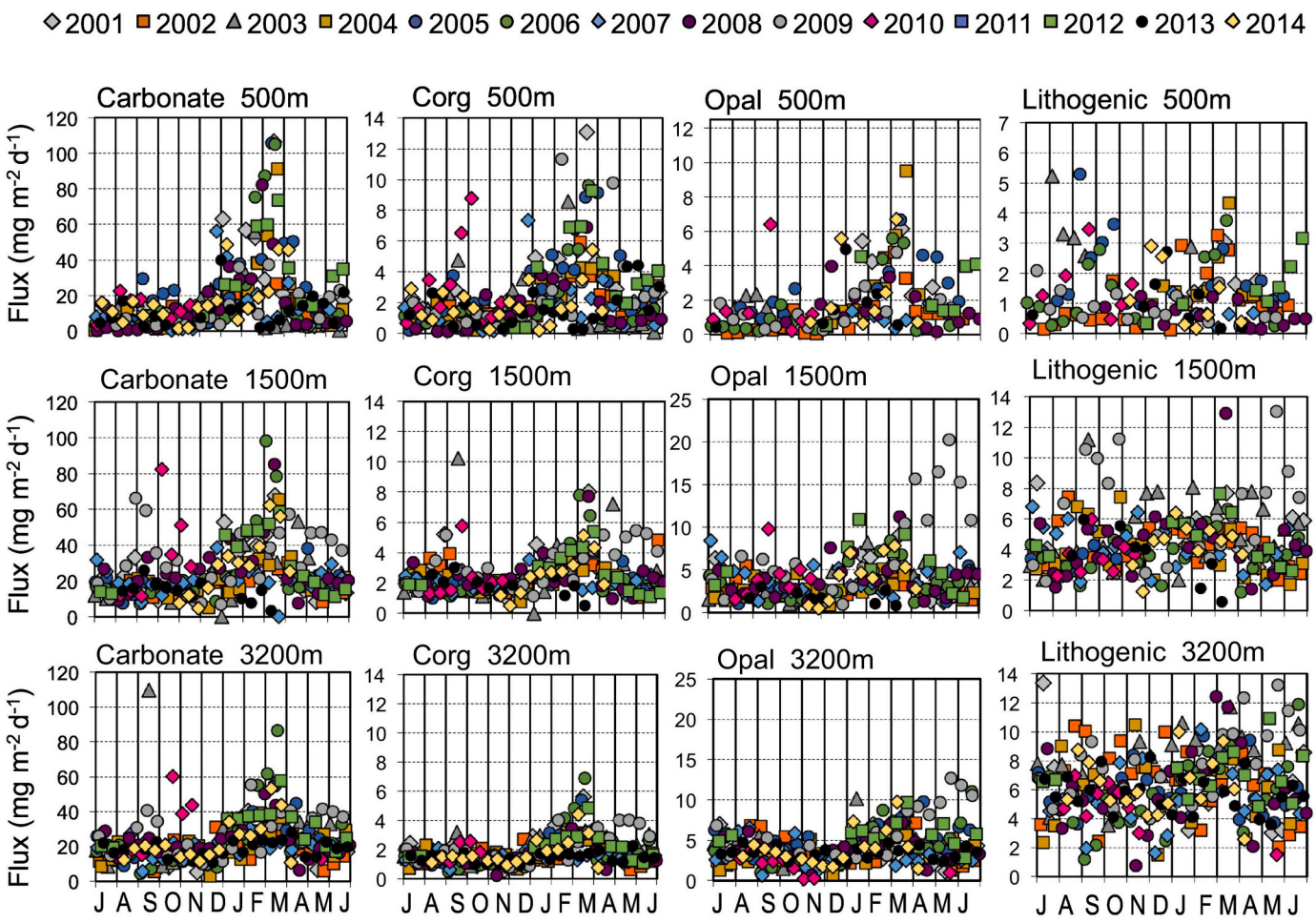

Fig. 6. Long term sediment trap particulate flux time series from the Bermuda Atlantic Time Series, showing seasonal variability in the flux of different particulate phases. Figure highlights the utility of time series data for investigating variability in particulate cycling, and is reproduced with permission from Conte et al. (2019).

and particulate TEI distributions have come new insights into our understanding of the physico-chemical speciation of TEIs in seawater. For example, while it has been known for a number of decades that organic ligands complex as much as 99% of dissolved Fe in seawater (see Gledhill and Buck, 2012), the GEOTRACES field program has led to the first high resolution ocean sections of both Fe-binding organic ligands and the size-partitioning of dissolved TEIs into soluble and colloidal species (e.g., Buck et al., 2015; Fitzsimmons et al., 2015; Gerringa et al., 2017; Roshan and Wu, 2018; Jensen et al., 2020). These studies yielded insights into the chemical characteristics of the phases binding Fe in seawater. Despite these advancements however, the molecular identity of most of the organic ligands in this pool remain uncharacterized. Several papers in this VSI add to our knowledge in this area. For example, González et al. classify diatom-produced polyphenol compounds in the laboratory as weak Fe-binding ligands, and add to the body of evidence that such organic Fe-binding ligands may reduce Fe (III) to release Fe(II) into seawater (González et al., 2019). At the other end of the Fe spectrum, Santana-González et al. use a novel approach to show how organic ligands influence Fe(II) to Fe(III) oxidation kinetics in a field study in the Labrador Sea, finding that while temperature, salinity, and pH are the driving variables influencing oxidation kinetics, organic matter can have both a positive and negative effect on reaction kinetics (Santana-González et al., 2019). Lastly, Lough et al. (2019) present a hydrothermal process study linking the role of ligands, colloids, and particles in controlling the speciation and longevity of Fe entering the ocean interior.

3. Outlook

What is beyond GEOTRACES? One obvious answer is provided by the GEOTRACES Science Plan, which points to section cruises stimulating new ideas and questions that may be answered by targeted laboratory and field process studies. We anticipate that this phase of the program will answer many questions raised by the section cruises. There is an urgent need for more studies on the processes influencing TEIs in high latitude regions where water masses form—the current paucity of data in these regions presents a key knowledge gap for understanding global cycling. A second answer is the development of programs which aim to link microbial activity directly to observed patterns of marine chemistry, such as the nascent 'BioGeoSCAPES' program. Lastly, we also look forward to new advances in analytical techniques which can further identify the chemical speciation, isotopic composition, and form of TEIs and organic molecules at even lower concentrations in the ocean.

Data sources for Table 1

Number of seawater samples presented per paper excludes replicate analyses of the same samples. *Cadmium:* 28, Lacan et al. (2006) 3, Ripperger and Rehkämper (2007); 22, Ripperger et al. (2007) 20, Abouchami et al. (2011); 2, Boyle et al. (2012); 51, Gault-Ringold and Stirling (2012); 11, Xue et al. (2012); 16, Yang et al. (2012); 12, Conway et al. (2013); 48, Xue et al. (2013); 53, Abouchami et al. (2014); 16, Yang et al. (2014); 516, 22, Conway and John (2015a, 2015b); 122, Janssen et al. (2017); 77, Xie et al. (2017); 69, Guinoiseau et al. (2019); 510,

John et al. (2018a); 134, Yang et al. (2018); 118, George et al. (2019); 158, 186, Sieber et al. (2019a, 2019b); 61, 82, Xie et al. (2019a, 2019b); 343, Zhang et al. (2019); 3, Hawco et al. (2020). *Iron:* 12, de Jong et al. (2007); 4, Lacan et al. (2008); 5, John and Adkins (2010); 16, Rouxel and Auro (2010); 11, Radic et al. (2011); 2 Boyle et al. (2012); 8, John and Adkins (2012); 31; John et al. (2012); 11, Conway et al. (2013); 11, Staubwasser et al. (2013); 468, Conway and John (2014b); 13, Labatut et al. (2014); 20, Ellwood et al. (2015); 286, Mawji et al. (2015); 12, Conway and John (2015b); 13, Chever et al. (2015); 12, Fitzsimmons et al. (2015); 41, Fitzsimmons et al. (2016); 34, Abadie et al. (2017); 57, Fitzsimmons et al. (2017); 12, Klar et al. (2017); 314, John et al. (2018b); 27, Klar et al. (2018); 65, Rolison et al. (2018); 164, Charette et al. (2020); 35, Ellwood et al. (2020); 20, Hawco et al. (2020). *Copper:* 7, Bermin et al. (2006); 25, Vance et al. (2008); 4, Boyle et al. (2012); 13, Takano et al. (2013); 9, Thompson et al. (2013); 77, Takano et al. (2014); 47, Thompson and Ellwood (2014); 17, Takano et al. (2017); 64, Little et al. (2018); 103, Baconnais et al. (2019); 20, Hawco et al. (2020); 48, Yang et al. (2020). *Zinc:* 7, Bermin et al. (2006); 7, John and Boyle (2007); 6, Boyle et al. (2012); 11, Conway et al. (2013); 569, Conway and John (2014a); 57, Zhao et al. (2014); 22, Conway and John (2015b); 30, Vance et al. (2016); 66, Samanta et al. (2017); 17, Takano et al. (2017); 526, John et al. (2018a); 26, Vance et al. (2019); 52, Wang et al. (2019a); 157, Charette et al. (2020); 35, Ellwood et al. (2020); 20, Hawco et al. (2020); 110, Lemaitre et al. (2020a); 121, Liao et al. (2020); 184, Sieber et al. (2020). *Nickel:* 29, Cameron and Vance (2014); 30, Vance et al. (2016); 17, Takano et al. (2017); 52, Wang et al. (2019b); 70, Archer et al. (2020); 19, Hawco et al. (2020); 49, Yang et al. (2020). *Chromium:* 9, Bonnand et al. (2013); 1, Paulukat et al. (2015); 29, Scheiderich et al. (2015); 1, Economou-Eliopoulos et al. (2016); 3, Holmden et al. (2016); 41, Paulukat et al. (2016); 3, Pereira et al. (2016); 4, Farkaš et al. (2018); 3, Frei et al. (2018); 43, Goring-Harford et al. (2018); 2, Bruggmann et al. (2019); 12, Moos and Boyle (2019); 66, Rickli et al. (2019); 5, Wang et al. (2019b); 5, Davidson et al. (2020); 41, Janssen et al. (2020); 25, Moos et al. (2020); 50, Nasemann et al. (2020).

Declaration of Competing Interest

The authors declare that they have no known competing financial interests or personal relationships that could have appeared to influence the work reported in this paper. None of the Guest Editors handled papers on which they were co-authors.

Acknowledgements

We thank the authors of all the articles in this VSI and express our immense gratitude to the large body of international GEOTRACES, CLIVAR, and SOLAS committee members, chief scientists, individual PIs, research staff, students, and national funding agencies who made the GEOTRACES revolution possible. We thank the other conveners of Session 10h (Christopher Pearce, Philip Pogge von Strandmann, Kathleen Scheiderich, and Juan Carlos Silva-Tamayo) and 10i (Geraldine Sarthou, Tianyu Chen, Gregory de Souza, Kristen Buck, Tina van de Flierdt, Walter Geibert, Zhimian Cao, Catherine Jeandel, and Phoebe Lam) in 2017, and all the authors who contributed to this VSI of *Chemical Geology*. We also thank J. Gerome who handled Moos et al. (2020); the *Chemical Geology* Editors in Chief, Michael Böttcher and Catherine Chauvel; and Tim Horscroft, Review Papers Coordinator at Elsevier Earth Science for facilitating this VSI. Tim Conway was supported by the University of South Florida.

References

Abadie, C., Lacan, F., Radic, A., Pradoux, C., Poitrasson, F., 2017. Iron isotopes reveal distinct dissolved iron sources and pathways in the intermediate versus deep Southern Ocean. Proc. Natl. Acad. Sci. U. S. A. 114, 858–863. https://doi.org/10.1073/pnas.1603107114.

Abouchami, W., Galer, S.J.G., de Baar, H.J.W., Alderkamp, A.C., Middag, R., Laan, P., Feldmann, H., Andreae, M.O., 2011. Modulation of the Southern Ocean cadmium isotope signature by ocean circulation and primary productivity. Earth Planet. Sci. Lett. 305, 83–91. https://doi.org/10.1016/j.epsl.2011.02.044.

Abouchami, W., Galer, S.J.G., de Baar, H.J.W., Middag, R., Vance, D., Zhao, Y., Klunder, M.B., Mezger, K., Feldmann, H., Andreae, M.O., 2014. Biogeochemical cycling of cadmium isotopes in the Southern Ocean along the Zero Meridian. Geochim. Cosmochim. Acta 127, 348–367. https://doi.org/10.1016/j.gca.2013.10.022.

Albarède, F., Goldstein, S.L., 1992. World map of Nd isotopes in sea-floor ferromanganese deposits. Geology 20 (8), 761–763. https://doi.org/10.1130/0091-7613(1992)020<0761:WMONII>2.3.CO;2.

Amakawa, H., Yu, T.L., Tazoe, H., Obata, H., Gamo, T., Sano, Y., Shen, C.C., Suzuki, K., 2019. Neodymium concentration and isotopic composition distributions in the southwestern Indian Ocean and the Indian sector of the Southern Ocean. Chem. Geol. 511, 190–203. VSI. https://doi.org/10.1016/j.chemgeo.2019.01.007.

Anderson, R.F., 2020. GEOTRACES: accelerating research on the marine biogeochemical cycles of trace elements and their isotopes. Annu. Rev. Mar. Sci. 12, 49–85. https://doi.org/10.1146/annurev-marine-010318-095123.

Anderson, R.F., Henderson, G.M., 2005. GEOTRACES a global study of the marine biogeochemical cycles of trace elements and their isotopes. Oceanography 18 (3), 76–79.

Anderson, R.F., Mawji, E., Cutter, G.C., Measures, C.I., Jeandel, C., 2014. GEOTRACES: Changing the way we explore ocean chemistry. Oceanography 27, 50–61.

Anderson, R.F., Cheng, H., Edwards, R.L., Fleisher, M.Q., Hayes, C.T., Huang, K.-F., Kadko, D., Lam, P.J., Landing, W.M., Lao, Y., Lu, Y., Measures, C.I., Moran, S.B., Morton, P.L., Ohnemus, D.C., Robinson, L.F., Shelley, R.U., 2016. How well can we quantify dust deposition to the ocean? Philos. Trans. R. Soc. Lond. A 374 (2081), 20150285.

Archer, C., Vance, D., Milne, A., Lohan, M.C., 2020. The oceanic biogeochemistry of nickel and its isotopes: new data from the South Atlantic and the Southern Ocean biogeochemical divide. Earth Planet. Sci. Lett. 535, 116118. https://doi.org/10.1016/j.epsl.2020.116118.

Arimoto, R., Duce, R.A., Ray, B.J., Ellis, W.G., Cullen, J.D., Merrill, J.T., 1995. Trace elements in the atmosphere over the North Atlantic. J. Geophys. Res. 100, 1199–1213. https://doi.org/10.1029/94JD02618.

Baars, O., Abouchami, W., Galer, S.J.G., Boye, M., Croot, P.L., 2014. Dissolved cadmium in the Southern Ocean: distribution, speciation, and relation to phosphate. Limnol. Oceanogr. 59, 385–399. https://doi.org/10.4319/lo.2014.59.2.0385.

Baconnais, I., Rouxel, O., Dulaquais, G., Boye, M., 2019. Determination of the copper isotope composition of seawater revisited: a case study from the Mediterranean Sea. Chem. Geol. 511, 465–480. VSI. https://doi.org/10.1016/j.chemgeo.2018.09.009.

Baker, A.R., Jickells, T.D., Witt, M., Linge, K.L., 2006. Trends in the solubility of iron, aluminium, manganese and phosphorus in aerosol collected over the Atlantic Ocean. Mar. Chem. 98, 43–58. https://doi.org/10.1016/j.marchem.2005.06.004.

Barraqueta, J.L.M., Klar, J., Gledhill, M., Schlosser, C., Shelley, R., Planquette, H.F., Wenzel, B., Sarthou, G., Achterberg, E., 2019. Atmospheric deposition fluxes over the Atlantic Ocean: A GEOTRACES case study. Biogeosciences 16, 1525–1542. https://doi.org/10.5194/bg-16-1525-2019.

Barrett, P.M., Resing, J.A., Grand, M.M., Measures, C.I., Landing, W.M., 2018. Trace element composition of suspended particulate matter along three meridional CLIVAR sections in the Indian and Southern Oceans: impact of scavenging on Al distributions. Chem. Geol. 502, 15–28. VSI. https://doi.org/10.1016/j.chemgeo.2018.06.015.

Bermin, J., Vance, D., Archer, C., Statham, P.J., 2006. The determination of the isotopic composition of Cu and Zn in seawater. Chem. Geol. 226, 280–297. https://doi.org/10.1016/j.chemgeo.2005.09.025.

Bishop, J.K.B., Lam, P.J., Wood, T.J., 2012. Getting good particles: accurate sampling of particles by large volume in-situ filtration. Limnol. Oceanogr. Methods 10, 681–710. https://doi.org/10.4319/lom.2012.10.681.

Bonnand, P., James, R.H., Parkinson, I.J., Connelly, D.P., Fairchild, I.J., 2013. The chromium isotopic composition of seawater and marine carbonates. Earth Planet. Sci. Lett. 382, 10–20. https://doi.org/10.1016/j.epsl.2013.09.001.

Boss, E., Guidi, L., Richardson, M.J., Stemmann, L., Gardner, W., Bishop, J.K.B., Anderson, R.F., Sherrell, R.M., 2015. Optical techniques for remote and in-situ characterization of particles pertinent to GEOTRACES. Prog. Oceanogr. 133, 43–54. https://doi.org/10.1016/j.pocean.2014.09.007.

Boyd, P.W., Ellwood, M.J., 2010. The biogeochemical cycle of iron in the ocean. Nat. Geosci. 3, 675–682. https://doi.org/10.1038/ngeo964.

Boyle, E.A., Sclater, F., Edmond, J.M., 1976. On the marine geochemistry of cadmium. Nature 263, 42–44.

Boyle, E.A., John, S.G., Abouchami, W., Adkins, J.F., Echegoyen-Sanz, Y., Ellwood, M.J., Flegal, A.R., Fornace, K., Gallon, C., Galer, S.J.G., 2012. GEOTRACES IC1 (BATS) contamination-prone trace element isotopes Cd, Fe, Pb, Zn, Cu, and Mo intercalibration. Limnol. Oceanogr. Methods 10, 653–665. https://doi.org/10.4319/lom.2012.10.653.

Broecker, W.S., Peng, T.-H., 1982. Tracers in the Sea. Lamont-Doherty Geological Observatory, Columbia University, Palisades, NY.

Bruggmann, S., Scholz, F., Klaebe, R.M., Canfield, D.E., Frei, R., 2019. Chromium isotope cycling in the water column and sediments of the Peruvian continental margin. Geochim. Cosmochim. Acta 257, 224–242. https://doi.org/10.1016/j.gca.2019.05.001.

Bruland, K.W., 1980. Oceanographic distributions of cadmium, zinc, nickel, and copper in the North Pacific. Earth Planet. Sci. Lett. 47, 176–198. https://doi.org/10.1016/0012-821X(80)90035-7.

Bruland, K.W., Knauer, G.A., Martin, J.H., 1978. Zinc in Northeast Pacific water. Nature 271, 741–743.
Buck, C.S., Landing, W.M., Resing, J.A., Lebon, G.T., 2006. Aerosol iron and aluminum solubility in the northwest Pacific Ocean: results from the 2002 IOC cruise. Geochem. Geophys. Geosyst. 7, 21 (doi: Q04m0710.1029/2005gc000977).
Buck, C.S., Landing, W.M., Resing, J.A., Measures, C.I., 2010. The solubility and deposition of aerosol Fe and other trace elements in the North Atlantic Ocean: observations from the A16N CLIVAR/CO2 repeat hydrography section. Mar. Chem. 120, 57–70. https://doi.org/10.1016/j.marchem.2008.08.003.
Buck, C.S., Landing, W.M., Resing, J., 2013. Pacific Ocean aerosols: deposition and solubility of iron, aluminum, and other trace elements. Mar. Chem. 157, 117–130. https://doi.org/10.1016/j.marchem.2013.09.005.
Buck, K., Sohst, B.M., Sedwick, P.N., 2015. The organic complexation of dissolved iron along the U.S. GEOTRACES (GA03) North Atlantic Section. Deep Sea Res. II 116, 152–165. https://doi.org/10.1016/j.dsr2.2014.11.016.
Buck, C.S., Aguilar-Islas, A., Marsay, C., Kadko, D., Landing, W.M., 2019. Trace element concentrations, elemental ratios, and enrichment factors observed in aerosol samples collected during the US GEOTRACES eastern Pacific Ocean transect (GP16). Chem. Geol. 511, 212–224. VSI. https://doi.org/10.1016/j.chemgeo.2019.01.002.
Cameron, V., Vance, D., 2014. Heavy nickel isotope compositions in rivers and the oceans. Geochim. Cosmochim. Acta 128, 195–211. https://doi.org/10.1016/j.gca.2013.12.007.
Charette, M.A., Dulaiova, H., Gonneea, M.E., Henderson, P.B., Moore, W.S., Scholten, J. C., Pham, M.K., 2012. GEOTRACES radium isotopes interlaboratory comparison experiment. Limnol. Oceanogr. Methods 10, 451–463. https://doi.org/10.4319/lom.2012.10.451.
Charette, M.A., Kipp, L.E., Jensen, L.T., Dabrowski, J.S., Whitmore, L.M., Fitzsimmons, J. N., Williford, T., Ulfsbo, A., Jones, E., Bundy, R.M., Vivancos, S.M., Pahnke, K., John, S.G., Xiang, Y., Hatta, M., Petrova, M.V., Heimbürger-Boavida, L.E., Bauch, D., Newton, R., Pasqualini, A., Agather, A.M., Amon, R.M.W., Anderson, R.F., Andersson, P.S., Benner, R., Bowman, K.L., Edwards, R.L., Gdaniec, S., Gerringa, L.J. A., González, A.G., Granskog, M., Haley, B., Hammerschmidt, C.R., Hansell, D.A., Henderson, P.B., Kadko, D.C., Kaiser, K., Laan, P., Lam, P.J., Lamborg, C.H., Levier, M., Li, X., Margolin, A.R., Measures, C., Middag, R., Millero, F.J., Moore, W. S., Paffrath, R., Planquette, H., Rabe, B., Reader, H., Rember, R., Rijkenberg, M.J.A., Roy-Barman, M., Rutgers van der Loeff, M., Saito, M., Schauer, U., Schlosser, P., Sherrell, R.M., Shiller, A.M., Slagter, H., Sonke, J.E., Stedmon, C., Woosley, R.J., Valk, O., van Ooijen, J., Zhang, R., 2020. The Transpolar Drift as a Source of Riverine and Shelf-Derived Trace Elements to the Central Arctic Ocean. J. Geophys. Res. Ocean 125. https://doi.org/10.1029/2019JC015920.
Charette, M.A., Morris, P.J., Henderson, P.B., Moore, W.S., 2015. Radium isotope distributions during the US GEOTRACES North Atlantic cruises. Mar. Chem. 177, 184–195. https://doi.org/10.1016/j.marchem.2015.01.001.
Charette, M.A., Lam, P.J., Lohan, M.C., Kwon, E.Y., Hatje, V., Jeandel, C., Shiller, A.M., Cutter, G.A., Thomas, A., Boyd, P.W., Homoky, W.B., Milne, A., Thomas, H., Andersson, P.S., Porcelli, D., Tanaka, T., Geibert, W., Dehairs, F., Garcia-Orellana, J., 2016. Coastal ocean and shelf-sea biogeochemical cycling of trace elements and isotopes: lessons learned from GEOTRACES. Philos. Trans. R. Soc. A 374 (2081), 20160076. https://doi.org/10.1098/rsta.2016.0076.
Cheize, M., Planquette, H.F., Fitzsimmons, J.N., Pelleter, E., Sherrell, R.M., Lambert, C., Bucciarelli, E., Sarthou, G., le Goff, M., Liorzou, C., Chéron, S., Viollier, E., Gayet, N., 2019. Contribution of resuspended sedimentary particles to dissolved iron and manganese in the ocean: an experimental study. Chem. Geol. 511, 389–415. VSI. https://doi.org/10.1016/j.chemgeo.2018.10.003.
Chever, F., Rouxel, O.J., Croot, P.L., Ponzevera, E., Wuttig, K., Auro, M.E., 2015. Total dissolvable and dissolved iron isotopes in the water column of the Peru upwelling regime. Geochim. Cosmochim. Acta 162. https://doi.org/10.1016/j.gca.2015.04.031.
Chien, C.T., Allen, B., Dimova, N.T., Yang, J., Reuter, J., Schladow, G., Paytan, A., 2019. Evaluation of atmospheric dry deposition as a source of nutrients and trace metals to Lake Tahoe. Chem. Geol. 511, 178–189. VSI. https://doi.org/10.1016/j.chemgeo.2019.02.005.
Chow, T.J., Goldberg, E.D., 1960. On the marine geochemistry of barium. Geochim. Cosmochim. Acta 20, 192–198. https://doi.org/10.1016/0016-7037(60)90073-9.
Church, T.M., Wolgemuth, K., 1972. Marine barite saturation. Earth Planet. Sci. Lett. 15, 35–44. https://doi.org/10.1016/0012-821X(72)90026-X.
Cloete, R., Loock, J.C., Mtshali, T., Fietz, S., Roychoudhury, A.N., 2019. Winter and summer distributions of Copper, Zinc and Nickel along the International GEOTRACES Section GIPY05: insights into deep winter mixing. Chem. Geol. 511, 342–357. VSI. https://doi.org/10.1016/j.chemgeo.2018.10.023.
Close, H.G., Lam, P.J., Popp, B.N., 2021. Marine particle chemistry: influence on biogeochemical cycles and particle export. ACS Earth Space Chem. 5 (5), 1210–1211. https://doi.org/10.1021/acsearthspacechem.1c00091.
Conte, M.H., Carter, A.M., Koweek, D.A., Huang, S., Weber, J.C., 2019. The elemental composition of the deep particle flux in the Sargasso Sea. Chem. Geol. 511, 279–313. VSI. https://doi.org/10.1016/j.chemgeo.2018.11.001.
Conway, T.M., John, S.G., 2014a. The biogeochemical cycling of zinc and zinc isotopes in the North Atlantic Ocean. Glob. Biogeochem. Cycles 28, 1111–1128. https://doi.org/10.1002/2014GB004862.
Conway, T.M., John, S.G., 2014b. Quantification of dissolved iron sources to the North Atlantic Ocean. Nature 511, 212–215. https://doi.org/10.1038/nature13482.
Conway, T.M., John, S.G., 2015a. Biogeochemical cycling of cadmium isotopes along a high-resolution section through the North Atlantic Ocean. Geochim. Cosmochim. Acta 148, 269–283. https://doi.org/10.1016/j.gca.2014.09.032.
Conway, T.M., John, S.G., 2015b. The cycling of iron, zinc and cadmium in the North East Pacific Ocean - insights from stable isotopes. Geochim. Cosmochim. Acta 164 (1), 262–283.
Conway, T.M., Rosenberg, A.D., Adkins, J.F., John, S.G., 2013. A new method for precise determination of iron, zinc and cadmium stable isotope ratios in seawater by double-spike mass spectrometry. Anal. Chim. Acta 793, 44–52. https://doi.org/10.1016/j.aca.2013.07.025.
Conway, T.M., John, S.G., Lacan, F., 2016. Intercomparison of dissolved iron isotope profiles from reoccupation of three GEOTRACES stations in the Atlantic Ocean. Mar. Chem. 183, 50–61.
Cutter, G.A., Bruland, K.W., 2012. Rapid and noncontaminating sampling system for trace elements in global ocean surveys. Limnol. Oceanogr. Methods 10, 425–436. https://doi.org/10.4319/lom.2012.10.425.
Cutter, G.A., Casciotti, K., Croot, P., Geibert, W., Heimbürger, L.E., Lohan, M.C., Planquette, H., van de Flierdt, T., 2017. Sampling and Sample-handling Protocols for GEOTRACES Cruises, Version 3.0. Bremerhaven, GEOTRACES Standards and Intercalibration Committee. https://epic.awi.de/id/eprint/51363/.
Davidson, A.B., Semeniuk, D.M., Koh, J., Holmden, C., Jaccard, S.L., Francois, R., Crowe, S.A., 2020. A $Mg(OH)_2$ coprecipitation method for determining chromium speciation and isotopic composition in seawater. Limnol. Oceanogr. Methods 18, 8–19. https://doi.org/10.1002/lom3.10342.
de Baar, H.J., Saager, P.M., Nolting, R.F., van der Meer, J., 1994. Cadmium versus phosphate in the world ocean. Mar. Chem. 46, 261–281. https://doi.org/10.1016/0304-4203(94)90082-5.
de Jong, J.T.M., Schoemann, V., Tison, J.-L., Becquevort, S., Masson, F., Lannuzel, D., Petit, J.C.J., Chou, L., Weiss, D.J., Mattielli, N., 2007. Precise measurement of Fe isotopes in marine samples by multi-collector inductively coupled plasma mass spectrometry (MC-ICP-MS). Anal. Chim. Acta 589, 105–119. https://doi.org/10.1016/j.aca.2007.02.055.
de Souza, G.F., Reynolds, B.C., Rickli, J., Frank, M., Saito, M.A., Gerringa, L.J.A., Bourdon, B., 2012a. Southern Ocean control of silicon stable isotope distribution in the deep Atlantic Ocean. Glob. Biogeochem. Cycles 26, GB2035. https://doi.org/10.1029/2011GB004141.
de Souza, G.F., Reynolds, B.C., Johnson, G.C., Bullister, J.L., Bourdon, B., 2012b. Silicon stable isotope distribution traces Southern Ocean export of Si to the eastern South Pacific thermocline. Biogeosciences 9, 4199–4213. https://doi.org/10.5194/bg-9-4199-2012.
Dehairs, F., Chesselet, R., Jedwab, J., 1980. Discrete suspended particles of barite and the barium cycle in the open ocean. Earth Planet. Sci. Lett. 49, 528–550. https://doi.org/10.1016/0012-821X(80)90094-1.
Deng, N., Stack, A.G., Weber, J., Cao, B., De Yoreo, J.J., Hu, Y., 2019. Organic–mineral interfacial chemistry drives heterogeneous nucleation of Sr-rich $(Ba_x, Sr_{1-x})SO_4$ from undersaturated solution. Proc. Natl. Acad. Sci. 116 (27), 13221–13226.
Duce, R.A., Tindale, N.W., 1991. Atmospheric transport of iron and its deposition in the ocean. Limnol. Oceanogr. 36, 1715–1726.
Duce, R.A., Liss, P.S., Merrill, J.T., Atlas, E.L., Buat-Menard, P., Hicks, B.B., Miller, J.M., Prospero, J.M., Arimoto, R., Church, T.M., Ellis, W., Galloway, J.N., Hansen, L., Jickells, T.D., Knap, A.H., Reinhardt, K.H., Schneider, B., Soudine, A., Tokos, J.J., Tsunogai, S., Wollast, R., Zhou, M., 1991. The atmospheric input of trace species to the world ocean. Glob. Biogeochem. Cycles 5, 193–259. https://doi.org/10.1029/91GB01778.
Economou-Eliopoulos, M., Frei, R., Megremi, I., 2016. Potential leaching of Cr(VI) from laterite mines and residues of metallurgical products (red mud and slag): an integrated approach. J. Geochem. Explor. 162, 40–49. https://doi.org/10.1016/j.gexplo.2015.12.007.
Ellwood, M.J., Hutchins, D.A., Lohan, M.C., Milne, A., Nasemann, P., Nodder, S.D., Sander, S.G., Strzepek, R.F., Wilhelm, S.W., Boyd, P.W., 2015. Iron stable isotopes track pelagic iron cycling during a subtropical phytoplankton bloom. Proc. Natl. Acad. Sci. U. S. A. 112, E15–E20. https://doi.org/10.1073/pnas.1421576112.
Ellwood, M.J., Strzepek, R.F., Strutton, P.G., Trull, T.W., Fourquez, M., Boyd, P.W., 2020. Distinct iron cycling in a Southern Ocean eddy. Nat. Commun. 11, 825. https://doi.org/10.1038/s41467-020-14464-0.
Farkaš, J., Frýda, J., Paulukat, C., Hathorne, E.C., Matoušková, Š., Rohovec, J., Frýdová, B., Francová, M., Frei, R., 2018. Chromium isotope fractionation between modern seawater and biogenic carbonates from the Great Barrier Reef, Australia: implications for the paleo-seawater δ53Cr reconstruction. Earth Planet. Sci. Lett. 498, 140–151. https://doi.org/10.1016/j.epsl.2018.06.032.
Fitzsimmons, J.N., Boyle, E.A., Jenkins, W.J., 2014. Distal transport of dissolved hydrothermal iron in the deep South Pacific Ocean. Proc. Natl. Acad. Sci. 111, 16654–16661. https://doi.org/10.1073/pnas.1418778111.
Fitzsimmons, J.N., Carrasco, G., Wu, J., Roshan, S., Hatta, M., Measures, C.I., Conway, T. M., John, S.G., Boyle, E.A., 2015. Partitioning of dissolved iron and iron isotopes into soluble and colloidal phases along the GA03 GEOTRACES North Atlantic Transect. Deep-Sea Res. II 116, 130–151. https://doi.org/10.1016/j.dsr2.2014.11.014.
Fitzsimmons, J.N., Conway, T.M., Lee, J.-M., Kayser, R., Thyng, K.M., John, S.G., Boyle, E.A., 2016. Dissolved iron and iron isotopes in the Southeastern Pacific Ocean. Glob. Biogeochem. Cycles 30 (10), 1372–1395.
Fitzsimmons, J.N., John, S.G., Marsay, C.M., Hoffman, C.L., Nicholas, S.L., Toner, B.M., German, C.R., Sherrell, R.M., 2017. Iron persistence in a distal hydrothermal plume supported by dissolved–particulate exchange. Nat. Geosci. 10, 195–201. https://doi.org/10.1038/ngeo2900.
Frank, M., 2002. Radiogenic isotopes: Tracers of past ocean circulation and erosional input. Rev. Geophys. 40 https://doi.org/10.1029/2000RG000094, 1-1-1–38.
Frank, M., Jeandel, C., Anderson, R.F., Henderson, G., Francos, R., Sharma, M., 2003. GEOTRACES: Studying the global marine biogeochemistry of trace elements and isotopes. Eos 84 (34), 327–330. https://doi.org/10.1029/2003EO340006.

Frei, R., Paulukat, C., Bruggmann, S., Klaebe, R.M., 2018. A systematic look at chromium isotopes in modern shells-implications for paleo-environmental reconstructions. Biogeosciences 15, 4905–4922. https://doi.org/10.5194/bg-15-4905-2018.

Frew, R.D., Hunter, K.A., 1992. Influence of Southern Ocean waters on the cadmium-phosphate properties of the global ocean. Nature 360, 144–146.

Garcia-Orellana, J., Rodellas, V., Tamborski, J., Diego-Feliu, M., van Beek, P., Weinstein, Y., Charette, M., Alorda-Kleinglass, A., Michael, H.A., Stieglitz, T., Scholten, J., 2021. Radium isotopes as submarine groundwater discharge (SGD) tracers: review and recommendations. Earth Sci. Rev., 103681 https://doi.org/10.1016/j.earscirev.2021.103681.

Gault-Ringold, M., Stirling, C.H., 2012. Anomalous isotopic shifts associated with organic resin residues during cadmium isotopic analysis by double spike MC-ICPMS. J. Anal. At. Spectrom. 27, 449. https://doi.org/10.1039/c2ja10360e.

George, E., Stirling, C.H., Gault-Ringold, M., Ellwood, M.J., Middag, R., 2019. Marine biogeochemical cycling of cadmium and cadmium isotopes in the extreme nutrient-depleted subtropical gyre of the South West Pacific Ocean. Earth Planet. Sci. Lett. 514, 84–95. https://doi.org/10.1016/j.epsl.2019.02.031.

GEOTRACES Planning Group, 2006. GEOTRACES Science Plan. Scientific Committee on Oceanic Research, Baltimore, Maryland.

Gerringa, L.J.A., Slagter, H.A., Bown, J., van Haren, H., Laan, P., de Baar, H.J.W., Rijkenberg, M.J.A., 2017. Dissolved Fe and Fe-binding organic ligands in the Mediterranean Sea – GEOTRACES G04. Mar. Chem. 194, 100–113. https://doi.org/10.1016/j.marchem.2017.05.012.

Gledhill, M., Buck, K., 2012. The organic complexation of iron in the marine environment: a review. Front. Microbiol. 3, 69. https://doi.org/10.3389/fmicb.2012.00069.

Goldstein, S.L., O'Nions, R.K., 1981. Nd and Sr isotopic relationships in pelagic clays and ferromanganese deposits. Nature 292, 324–327. https://doi.org/10.1038/292324a0.

González, A.G., Cadena-Aizaga, M.I., Sarthou, G., González-Dávila, M., Santana-Casiano, J.M., 2019. Iron complexation by phenolic ligands in seawater. Chem. Geol. 511, 380–388. VSI. https://doi.org/10.1016/j.chemgeo.2018.10.017.

Goring-Harford, H.J., Klar, J.K., Pearce, C.R., Connelly, D.P., Achterberg, E.P., James, R. H., 2018. Behaviour of chromium isotopes in the eastern sub-tropical Atlantic Oxygen Minimum Zone. Geochim. Cosmochim. Acta 236, 41–59. https://doi.org/10.1016/j.gca.2018.03.004.

Gourain, A., Planquette, H., Cheize, M., Lemaitre, N., Menzel Barraqueta, J.L., Shelley, R., Lherminier, P., Planquette, H., 2019. Inputs and processes affecting the distribution of particulate iron in the North Atlantic along the GEOVIDE (GEOTRACES GA01) section. Biogeosciences 16, 1563–1582. https://doi.org/10.5194/bg-16-1563-2019.

Grand, M.M., Buck, C.S., Landing, W.M., Measures, C.I., Hatta, M., Hiscock, W.T., Brown, M., 2014. Quantifying the Impact of Atmospheric Deposition on the Biogeochemistry of Fe and Al in the Upper Ocean: A Decade of Collaboration with the US CLIVAR-CO2. Repeat Hydrography Program 27, 62–65. https://doi.org/10.2307/24862119.

Guinoiseau, D., Galer, S.J.G., Abouchami, W., Frank, M., Achterberg, E.P., Haug, G.H., 2019. Importance of cadmium sulfides for biogeochemical cycling of Cd and its isotopes in oxygen deficient zones—a case study of the Angola Basin. Glob. Biogeochem. Cycles 33, 1746–1763. https://doi.org/10.1029/2019GB006323.

Hawco, N.J., Yang, S.C., Foreman, R.K., Funkey, C.P., Dugenne, M., White, A.E., Wilson, S.T., Kelly, R.L., Bian, X., Huang, K.F., Karl, D.M., John, S.G., 2020. Metal isotope signatures from lava-seawater interaction during the 2018 eruption of Kīlauea. Geochim. Cosmochim. Acta 282, 340–356. https://doi.org/10.1016/j.gca.2020.05.005.

Hayes, C.T., Anderson, R.F., Fleisher, M.Q., Vivancos, S.M., Lam, P.J., Ohnemus, D.C., Huang, K.F., Robinson, L.F., Lu, Y., Cheng, H., Edwards, R.L., Moran, S.B., 2015. Intensity of Th and Pa scavenging partitioned by particle chemistry in the North Atlantic Ocean. Mar. Chem. 170, 49–60. https://doi.org/10.1016/j.marchem.2015.01.006.

Hayes, C.T., Anderson, R.F., Cheng, H., Conway, T.M., Edwards, L., Fleisher, M.Q., Huang, K.-F., John, S.G., Landing, W.M., Little, S.H., Lu, Y., Morton, P.L., Moran, B., Robinson, L.F., Shelley, R.U., Shiller, A.M., Zheng, X., 2018. Replacement times of a spectrum of elements in the North Atlantic based on thorium supply. Glob. Biogeochem. Cycles 32, 1294–1311.

Hayes, C.T., Costa, K.M., Anderson, R.F., Calvo, E., Chase, Z., Demina, L.L., Dutay, J., German, C.R., Heimbürger-Boavida, L., Jaccard, S.L., Jacobel, A., Kohfeld, K.E., Kravchishina, M.D., Lippold, J., Mekik, F., Missiaen, L., Pavia, F.J., Paytan, A., Pedrosa-Pamies, R., Petrova, M.V., Rahman, S., Robinson, L.F., Roy-Barman, M., Sanchez-Vidal, A., Shiller, A., Tagliabue, A., Tessin, A.C., van Hulten, M., Zhang, J., 2021. Global ocean sediment composition and burial flux in the Deep Sea. Global Biogeochem. Cycles 35. https://doi.org/10.1029/2020gb006769 e2020GB006769.

Henderson, G.M., 2016. Ocean trace element cycles. Philos. Trans. R. Soc. A 374. https://doi.org/10.1098/rsta.2015.0300, 2081, 20150300.

Henderson, P.B., Morris, P.J., Moore, W.S., Charette, M.A., 2013. Methodological advances for measuring low-level radium isotopes in seawater. J. Radioanal. Nuclear Chem. 357–362. https://doi.org/10.1007/s10967-012-2047-9.

Holmden, C., Jacobson, A.D., Sageman, B.B., Hurtgen, M.T., 2016. Response of the Cr isotope proxy to Cretaceous Ocean Anoxic Event 2 in a pelagic carbonate succession from the Western Interior Seaway. Geochim. Cosmochim. Acta 186, 277–295. https://doi.org/10.1016/j.gca.2016.04.039.

Horner, T.J., Kinsley, C.W., Nielsen, S.G., 2015. Barium-isotopic fractionation in seawater mediated by barite cycling and oceanic circulation. Earth Planet. Sci. Lett. 430, 511–522. https://doi.org/10.1016/j.epsl.2015.07.027.

Horner, T.J., Pryer, H.V., Nielsen, S.G., Crockford, P.W., Gauglitz, J.M., Wing, B.A., Ricketts, R.D., 2017. Pelagic barite precipitation at micromolar ambient sulfate. Nat. Commun. 8, 1–11. https://doi.org/10.1038/s41467-017-01229-5.

Horner, T.J., Little, S.H., Conway, T.M., Farmer, J.R., Hertzberg, J.E., Janssen, D.J., Lough, A.J.M., Mckay, J., Tessin, A., Galer, S.J.G., Jaccard, S.L., Lacan, F., Paytan, A., Wuttig, K., GEOTRACES–PAGES Biological Productivity Working Group Members, 2021. Bioactive trace metals and their isotopes as paleoproductivity proxies: an assessment using GEOTRACES-era data. Glob. Biogeochem. Cycles, e2020GB006814. https://doi.org/10.1029/2020GB006814.

Janssen, D.J., Conway, T.M., John, S.G., Christian, J.R., Kramer, D.I., Pedersen, T.F., Cullen, J.T., 2014. Undocumented water column sink for cadmium in open ocean oxygen-deficient zones. Proc. Natl. Acad. Sci. U. S. A. 111, 6888–6893. https://doi.org/10.1073/pnas.1402388111.

Janssen, D.J., Abouchami, W., Galer, S.J.G., Cullen, J.T., 2017. Fine-scale spatial and interannual cadmium isotope variability in the subarctic northeast Pacific. Earth Planet Sci. Lett. 472, 241–252. https://doi.org/10.1016/j.epsl.2017.04.048.

Janssen, D.J., Rickli, J., Quay, P.D., White, A.E., Nasemann, P., Jaccard, S.L., 2020. Biological control of chromium redox and stable isotope composition in the surface ocean. Global Biogeochem. Cycles 34. https://doi.org/10.1029/2019GB006397 e2019GB006397.

Jeandel, C., 2016. Overview of the mechanisms that could explain the "Boundary Exchange" at the land-ocean contact. Philos. Trans. R. Soc. A 374 (2081), 20150287. https://doi.org/10.1098/rsta.2015.0287.

Jeandel, C., Arsouze, T., Lacan, F., Téchiné, P., Dutay, J.C., 2007. Isotopic Nd compositions and concentrations of the lithogenic inputs into the ocean: a compilation, with an emphasis on the margins. Chem. Geol. 239, 156–164. https://doi.org/10.1016/j.chemgeo.2006.11.013.

Jeandel, C., Rutgers van der Loeff, M., Lam, P.J., Roy-Barman, M., Sherrell, R.M., Kretschmer, S., German, C., Dehairs, F., 2015. What did we learn about ocean particle dynamics in the GEOSECS-JGOFS era? Prog. Oceanogr. 133, 6–16. https://doi.org/10.1016/j.pocean.2014.12.018.

Jensen, L.T., Morton, P., Twining, B.S., Heller, M.I., Hatta, M., Measures, C.I., John, S.G., Zhang, R., Pinedo-Gonzalez, P., Sherrell, R.M., Fitzsimmons, J.N., 2020. A comparison of marine Fe and Mn cycling: U.S. GEOTRACES GN01 Western Arctic case study. Geochim. Cosmochim. Acta 288, 138–160. https://doi.org/10.1016/j.gca.2020.08.006.

Jickells, T.D., An, Z.S., Andersen, K.K., Baker, A.R., Bergametti, C., Brooks, N., Cao, J.J., Boyd, P.W., Duce, R.A., Hunter, K.A., Kawahata, H., Kubilay, N., LaRoche, J., Liss, P. S., Mahowald, N., Prospero, J.M., Ridgwell, A.J., Tegen, I., Torres, R., 2005. Global iron connections between desert dust, ocean biogeochemistry, and climate. Science. https://doi.org/10.1126/science.1105959.

Jickells, T.D., Baker, A.R., Chance, R., 2016. Atmospheric transport of trace elements and nutrients to the oceans. Philos. Trans. R. Soc. A 374. https://doi.org/10.1098/rsta.2015.0286, 2081, 20150286.

John, S.G., Adkins, J.F., 2010. Analysis of dissolved iron isotopes in seawater. Mar. Chem. 119, 65–76. https://doi.org/10.1016/j.marchem.2010.01.001.

John, S.G., Adkins, J.F., 2012. The vertical distribution of iron stable isotopes in the North Atlantic near Bermuda. Glob. Biogeochem. Cycles 26, GB2034.

John, S.G., Boyle, E.A., 2007. Marine Biogeochemistry of Zinc Isotopes. Ph.D. Thesis Jt. Progr. Chem. Oceanogr. Woods Hole Oceanographic Institution / Massachusetts Institute of Technology.

John, S.G., Conway, T.M., 2014. A role for scavenging in the marine biogeochemical cycling of zinc and zinc isotopes. Earth Planet. Sci. Lett. 394, 159–167. https://doi.org/10.1016/j.epsl.2014.02.053.

John, S.G., Geis, R.W., Saito, M.A., Boyle, E.A., 2007. Zinc isotope fractionation during high-affinity and low-affinity zinc transport by the marine diatom Thalassiosira oceanica. Limnol. Oceanogr. 52, 2710–2714.

John, S.G., Mendez, J., Moffett, J.W., Adkins, J.F., 2012. The flux of iron and iron isotopes from San Pedro Basin sediments. Geochim. Cosmochim. Acta 93, 14–29. https://doi.org/10.1016/j.gca.2012.06.003.

John, S.G., Helgoe, J., Townsend, E., 2018a. Biogeochemical cycling of Zn and Cd and their stable isotopes in the Eastern Tropical South Pacific. Mar. Chem. 201, 256–262. https://doi.org/10.1016/j.marchem.2017.06.001.

John, S.G., Helgoe, J., Townsend, E., Weber, T., DeVries, T., Tagliabue, A., Moore, K., Lam, P., Marsay, C.M., Till, C., 2018b. Biogeochemical cycling of Fe and Fe stable isotopes in the Eastern Tropical South Pacific. Mar. Chem. 201, 66–76. https://doi.org/10.1016/J.MARCHEM.2017.06.003.

Johnson, K.S., Michael Gordon, R., Coale, K.H., 1997. What controls dissolved iron concentrations in the world ocean? Mar. Chem. 57 (3-4), 137–161. https://doi.org/10.1016/S0304-4203(97)00043-1.

Johnson, K.S., Boyle, E.A., Bruland, K.W., Coale, K.H., Measures, C.I., Moffett, J.W., Aguilar-Islas, A.M., Barbeau, K., Bergquist, B.A., Bowie, A.R., Buck, K., Cai, Y., Chase, Z., Cullen, J.T., Doi, T., Elrod, V.A., Fitzwater, S., Gordon, M., King, A., Laan, P., Laglera-Baquer, L., Landing, W.M., Lohan, M.C., Mendez, J., Milne, A., Obata, H., Ossiander, L., Plant, J.N., Sarthou, G., Sedwick, P.N., Smith, G.J., Sohst, B. M., Tanner, S., Van den Berg, Stan, Wu, J.F., Baquer, L., Landing, W.M., Lohan, M.C., Mendez, J., Milne, A., Obata, H., Ossiander, L., Plant, J.N., Sarthou, G., Sedwick, P. N., Smith, G.J., Sohst, B.M., Tanner, S., Van den Berg, S., Wu, J.F., 2007. Developing standards for dissolved iron in seawater. Eos 88, 131–132. https://doi.org/10.1029/2007EO110003.

Kipp, L.E., Sanial, V., Henderson, P.B., van Beek, P., Reyss, J.L., Hammond, D.E., Moore, W.S., Charette, M.A., 2018. Radium isotopes as tracers of hydrothermal inputs and neutrally buoyant plume dynamics in the deep ocean. Mar. Chem. 201, 51–65. https://doi.org/10.1016/j.marchem.2017.06.011.

Kipp, L.E., Kadko, D.C., Pickart, R.S., Henderson, P.B., Moore, W.S., Charette, M.A., 2019. Shelf-Basin interactions and water mass residence times in the Western Arctic

Ocean: insights provided by radium isotopes. J. Geophys. Res. Ocean 124, 3279–3297. https://doi.org/10.1029/2019JC014988.
Klar, J.K., James, R.H., Gibbs, D., Lough, A., Parkinson, I., Milton, J.A., Hawkes, J.A., Connelly, D.P., 2017. Isotopic signature of dissolved iron delivered to the Southern Ocean from hydrothermal vents in the East Scotia Sea. Geology 45, 351–354. https://doi.org/10.1130/G38432.1.
Klar, J.K., Schlosser, C., Milton, J.A., Woodward, E.M.S., Lacan, F., Parkinson, I.J., Achterberg, E.P., James, R.H., 2018. Sources of dissolved iron to oxygen minimum zone waters on the Senegalese continental margin in the tropical North Atlantic Ocean: insights from iron isotopes. Geochim. Cosmochim. Acta 236, 60–78. https://doi.org/10.1016/j.gca.2018.02.031.
Köbberich, M., Vance, D., 2017. Kinetic control on Zn isotope signatures recorded in marine diatoms. Geochim. Cosmochim. Acta 210, 97–113. https://doi.org/10.1016/j.gca.2017.04.014.
Köbberich, M., Vance, D., 2018. Zinc association with surface-bound iron-hydroxides on cultured marine diatoms: A zinc stable isotope perspective. Mar. Chem. 202, 1–11. https://doi.org/10.1016/j.marchem.2018.01.002.
Köbberich, M., Vance, D., 2019. Zn isotope fractionation during uptake into marine phytoplankton: implications for oceanic zinc isotopes. Chem. Geol. 523, 154–161. VSI. https://doi.org/10.1016/j.chemgeo.2019.04.004.
Kwon, E.Y., Kim, G., Primeau, F., Moore, W.S., Cho, H.M., Devries, T., Sarmiento, J.L., Charette, M.A., Cho, Y.K., 2014. Global estimate of submarine groundwater discharge based on an observationally constrained radium isotope model. Geophys. Res. Lett. 41, 8438–8444. https://doi.org/10.1002/2014GL061574.
Labatut, M., Lacan, F., Pradoux, C., Chmeleff, J., Radic, A., Murray, J.W., Poitrasson, F., Johansen, A.M., Thil, F., 2014. Iron sources and dissolved-particulate interactions in the seawater of the Western Equatorial Pacific, iron isotope perspectives. Glob. Biogeochem. Cycles 28, 1044–1065. https://doi.org/10.1002/2014GB004928.
Lacan, F., Jeandel, C., 2005. Neodymium isotopes as a new tool for quantifying exchange fluxes at the continent-ocean interface. Earth Planet. Sci. Lett. 232, 245–257. https://doi.org/10.1016/j.epsl.2005.01.004.
Lacan, F., Francois, R., Ji, Y., Sherrell, R., 2006. Cadmium isotopic composition in the ocean. Geochim. Cosmochim. Acta 70, 5104–5118. https://doi.org/10.1016/j.gca.2006.07.036.
Lacan, F., Radic, A., Jeandel, C., Poitrasson, F., Sarthou, G., Pradoux, C., Freydier, R., 2008. Measurement of the isotopic composition of dissolved iron in the open ocean. Geophys. Res. Lett. 35, L24610 https://doi.org/10.1029/2008GL035841.
Lacan, F., Radic, A., Labatut, M., Jeandel, C., Poitrasson, F., Sarthou, G., Pradoux, C., Chmeleff, J., Freydier, R., 2010. High-precision determination of the isotopic composition of dissolved iron in iron depleted seawater by double spike multicollector-ICPMS. Anal. Chem. 82, 7103–7111. https://doi.org/10.1021/ac1002504.
Lacan, F., Tachikawa, K., Jeandel, C., 2012. Neodymium isotopic composition of the oceans: a compilation of seawater data. Chem. Geol. 300–301, 177–184. https://doi.org/10.1016/j.chemgeo.2012.01.019.
Lagerström, M.E., Field, M.P., Séguret, M., Fischer, L., Hann, S., Sherrell, R.M., 2013. Automated on-line flow-injection ICP-MS determination of trace metals (Mn, Fe, Co, Ni, Cu and Zn) in open ocean seawater: application to the GEOTRACES program. Mar. Chem. 155, 71–80. https://doi.org/10.1016/j.marchem.2013.06.001.
Lam, P.J., Anderson, R.F., 2018. GEOTRACES: the marine biogeochemical cycle of trace elements and their isotopes. Elements 14, 377–378. https://doi.org/10.2138/gselements.14.6.377.
Lam, P.J., Twining, B.S., Jeandel, C., Roychoudhury, A., Resing, J., Santschi, P.H., Anderson, R.F., 2015a. Methods for analyzing the concentration and speciation of major and trace elements in marine particles. Prog. Oceanogr. doi. https://doi.org/10.1016/j.pocean.2015.01.005.
Lam, P.J., Ohnemus, D.C., Auro, M.E., 2015b. Size-fractionated major particle composition and concentrations from the US GEOTRACES North Atlantic Zonal Transect. Deep Sea Res. II 116, 303–320. https://doi.org/10.1016/j.dsr2.2014.11.020.
Lam, P.J., Lee, J.M., Heller, M.I., Mehic, S., Xiang, Y., Bates, N.R., 2018. Size-fractionated distributions of suspended particle concentration and major phase composition from the U.S. GEOTRACES Eastern Pacific Zonal Transect (GP16). Mar. Chem. 201, 90–107. https://doi.org/10.1016/j.marchem.2017.08.013.
Lambelet, M., van de Flierdt, T., Crocket, K., Rehkämper, M., Kreissig, K., Coles, B., Rijkenberg, M.J.A., Gerringa, L.J.A., de Baar, H.J.W., Steinfeldt, R., 2016. Neodymium isotopic composition and concentration in the western North Atlantic Ocean: results from the GEOTRACES GA02 section. Geochim. Cosmochim. Acta. https://doi.org/10.1016/j.gca.2015.12.019. In Press.
Laukert, G., Makhotin, M., Petrova, M.v., Frank, M., Hathorne, E.C., Bauch, D., Böning, P., Kassens, H., 2019. Water mass transformation in the Barents Sea inferred from radiogenic neodymium isotopes, rare earth elements and stable oxygen isotopes. Chem. Geol. 511, 416–430. VSI. https://doi.org/10.1016/j.chemgeo.2018.10.002.
Lemaitre, N., de Souza, G.F., Archer, C., Wang, R.M., Planquette, H., Sarthou, G., Vance, D., 2020a. Pervasive sources of isotopically light zinc in the North Atlantic Ocean. Earth Planet. Sci. Lett. 539, 116216. https://doi.org/10.1016/j.epsl.2020.116216.
Lemaitre, N., Planquette, H., Dehairs, F., Planchon, F., Sarthou, G., Gallinari, M., Roig, S., Jeandel, C., Castrillejo, M., 2020b. Particulate trace element export in the North Atlantic (GEOTRACES GA01 Transect, GEOVIDE Cruise). ACS Earth Space Chem. 4, 2185–2204. https://doi.org/10.1021/acsearthspacechem.0c00045.
Lenstra, W.K., Hermans, M., Séguret, M.J.M., Witbaard, R., Behrends, T., Dijkstra, N., van Helmond, N.A.G.M., Kraal, P., Laan, P., Rijkenberg, M.J.A., Severmann, S., Teacă, A., Slomp, C.P., 2019. The shelf-to-basin iron shuttle in the Black Sea revisited. Chem. Geol. 511, 314–341. VSI. https://doi.org/10.1016/j.chemgeo.2018.10.024.
Liao, W., Takano, S., Yang, S., Huang, K., Sohrin, Y., Ho, T., 2020. Zn isotope composition in the water column of the Northwestern Pacific Ocean: the importance of external sources. Global Biogeochem. Cycles. https://doi.org/10.1029/2019GB006379, 2019GB006379.
Little, S.H., Archer, C., Milne, A., Schlosser, C., Achterberg, E.P., Lohan, M.C., Vance, D., 2018. Paired dissolved and particulate phase Cu isotope distributions in the South Atlantic. Chem. Geol. 502, 29–43. VSI. https://doi.org/10.1016/j.chemgeo.2018.07.022.
Lohan, M.C., Aguilar-Islas, A.M., Franks, R.P., Bruland, K.W., 2005. Determination of iron and copper in seawater at pH 1.7 with a new commercially available chelating resin, NTA Superflow. Anal. Chim. Acta 530, 121–129.
López-Sánchez, D.E., Cobelo-García, A., Rijkenberg, M.J.A., Gerringa, L.J.A., de Baar, H.J.W., 2019. New insights on the dissolved platinum behavior in the Atlantic Ocean. Chem. Geol. 511, 204–211. VSI. https://doi.org/10.1016/j.chemgeo.2019.01.003.
Lough, A.J.M., Homoky, W.B., Connelly, D.P., Comer-Warner, S.A., Nakamura, K., Abyaneh, M.K., Kaulich, B., Mills, R.A., 2019. Soluble iron conservation and colloidal iron dynamics in a hydrothermal plume. Chem. Geol. 511, 225–237. VSI. https://doi.org/10.1016/j.chemgeo.2019.01.001.
Marinov, I., Gnanadesikan, A., Toggweiler, J.R., Sarminento, J.L., 2006. The Southern Ocean biogeochemical divide. Nature 441, 964–967.
Marsay, C.M., Kadko, D., Landing, W.M., Morton, P.L., Summers, B.A., Buck, C.S., 2018. Concentrations, provenance and flux of aerosol trace elements during US GEOTRACES Western Arctic cruise GN01. Chem. Geol. 502, 1–14. VSI. https://doi.org/10.1016/j.chemgeo.2018.06.007.
Martinez-Ruiz, F., Paytan, A., Gonzalez-Muñoz, M.T., Jroundi, F., Abad, M.M., Lam, P.J., Bishop, J.K.B., Horner, T.J., Morton, P.L., Kastner, M., 2019. Barite formation in the ocean: origin of amorphous and crystalline precipitates. Chem. Geol. 511, 441–451. VSI. https://doi.org/10.1016/j.chemgeo.2018.09.011.
Martinez-Ruiz, F., Paytan, A., Gonzalez-Muñoz, M.T., Jroundi, F., Abad, M.M., Lam, P.J., Horner, T.J., Kastner, M., 2020. Barite precipitation on suspended organic matter in the mesopelagic zone. Front. Earth Sci. 8. https://doi.org/10.3389/feart.2020.567714.
Mawji, E., Schlitzer, R., Dodas, E.M., Abadie, C., Abouchami, W., Anderson, R.F., Baars, O., Bakker, K., Baskaran, M., Bates, N.R., Bluhm, K., Bowie, A., Bown, J., Boye, M., Boyle, E.A., Branellec, P., Bruland, K.W., Brzezinski, M.A., Bucciarelli, E., Buesseler, K., Butler, E., Cai, P., Cardinal, D., Casciotti, K., Chaves, J., Cheng, H., Chever, F., Church, T.M., Colman, A.S., Conway, T.M., Croot, P.L., Cutter, G.A., de Baar, H.J.W., de Souza, G.F., Dehairs, F., Deng, F., Dieu, H.T., Dulaquais, G., Echegoyen-Sanz, Y., Lawrence Edwards, R., Fahrbach, E., Fitzsimmons, J., Fleisher, M., Frank, M., Friedrich, J., Fripiat, F., Galer, S.S.J.G., Gamo, T., Solsona, E.G., Gerringa, L.J.A., Godoy, J.M., Gonzalez, S., Grossteffan, E., Hattaa, M., Hayes, C.T., Heller, M.I., Henderson, G., Huang, K.-F., Jeandel, C., Jenkins, W.J., John, S.G., Kenna, T.C., Klunder, M., Kretschmer, S., Kumamoto, Y., Laan, P., Labatut, M., Lacan, F., Lam, P.J., Lannuzel, D., le Moigne, F., Lechtenfeld, O.J., Lohan, M.C., Lua, Y., Masqué, P., McClain, C.R., Measures, C., Middag, R., Moffett, J., Navidad, A., Nishioka, J., Noble, A., Obata, H., Ohnemus, D.C., Owens, S., Planchon, F., Pradoux, C., Puigcorbé, V., Quaya, P., Radic, A., Rehkämper, M., Remenyi, T., Rijkenberg, M.J.A., Rintoul, S., Robinson, L.F., Roeske, T., Rosenberg, M., van der Loeff, M.R., Ryabenko, E., Saito, M.A., Roshan, S., Salt, L., Sarthou, G., Schauer, U., Scott, P., Sedwick, P.N., Sha, L., Shiller, A.M., Sigman, D.M., Smethie, W., Smith, G.J., Sohrin, Y., Speich, S., Stichel, T., Stutsman, J., Swift, J.H., Tagliabue, A., Thomas, A., Tsunogai, U., Twining, B.S., van Aken, H.M., van Heuven, S., van Ooijen, J., van Weerlee, E., Venchiarutti, C., Voelker, A.H.L., Wake, B., Warner, M.J., Woodward, E.M.S., Wu, J., Wyatt, N., Yoshikawa, H., Zheng, X.-Y., Xue, Z., Zieringer, M., Zimmer, L.A., Hatta, M., Lu, Y., Quay, P., 2015. The GEOTRACES intermediate data product 2014. Mar. Chem. 177, 1–8. https://doi.org/10.1016/j.marchem.2015.04.005.
Mayfield, K.K., Eisenhauer, A., Santiago Ramos, D.P., Higgins, J.A., Horner, T.J., Auro, M., Magna, T., Moosdorf, N., Charette, M.A., Gonneea, M.E., Brady, C.E., Komar, N., Peucker-Ehrenbrink, B., Paytan, A., 2021. Groundwater discharge impacts marine isotope budgets of Li, Mg, Ca, Sr, and Ba. Nat. Commun. 12, 1–9. https://doi.org/10.1038/s41467-020-20248-3.
McDonnell, A.M.P., Lam, P.J., Lamborg, C.H., Buesseler, K.O., Sanders, R., Riley, J.S., Marsay, C., Smith, H.E.K., Sargent, E.C., Lampitt, R.S., Bishop, J.K.B., 2015. The oceanographic toolbox for the collection of sinking and suspended marine particles. Prog. Oceanogr. 133, 17–31. https://doi.org/10.1016/j.pocean.2015.01.007.
Middag, R., Sefarian, R., Conway, T.M., John, S.G., Bruland, K.W., de Baar, H.J.W., 2015. Intercomparison of dissolved trace elements at the Bermuda Atlantic Time Series Station. Mar. Chem. 177 (3), 476–479.
Middag, R., van Heuven, S.M.A.C., Bruland, K.W., de Baar, H.J.W., 2018. The relationship between cadmium and phosphate in the Atlantic Ocean unravelled. Earth Planet. Sci. Lett. 492, 79–88. https://doi.org/10.1016/j.epsl.2018.03.046.
Moffett, J.W., German, C.R., 2020. Distribution of iron in the Western Indian Ocean and the Eastern tropical South pacific: an inter-basin comparison. Chem. Geol. 532 https://doi.org/10.1016/j.chemgeo.2019.119334. VSI.
Moore, W.S., 1969. Oceanic concentrations of ^{228}Radium. Earth Planet. Sci. Lett. 6, 437–446. https://doi.org/10.1016/0012-821x(69)90113-7.
Moore, W.S., 2000. Determining coastal mixing rates using radium isotopes. Cont. Shelf Res. 20, 1993–2007. https://doi.org/10.1016/S0278-4343(00)00054-6.
Moore, W.S., Shaw, T.J., 2008. Fluxes and behavior of radium isotopes, barium, and uranium in seven Southeastern US rivers and estuaries. Mar. Chem. 108, 236–254. https://doi.org/10.1016/j.marchem.2007.03.004.

Moore, W.S., Ussler, W., Paull, C.K., 2008. Short-lived radium isotopes in the Hawaiian margin: evidence for large fluid fluxes through the Puna Ridge. Mar. Chem. 109, 421–430. https://doi.org/10.1016/j.marchem.2007.09.010.

Moos, S.B., Boyle, E.A., 2019. Determination of accurate and precise chromium isotope ratios in seawater samples by MC-ICP-MS illustrated by analysis of SAFe Station in the North Pacific Ocean. Chem. Geol. 511, 481–493. VSI. https://doi.org/10.1016/j.chemgeo.2018.07.027.

Moos, S.B., Boyle, E.A., Altabet, M.A., Bourbonnais, A., 2020. Investigating the cycling of chromium in the oxygen deficient waters of the Eastern Tropical North Pacific Ocean and the Santa Barbara Basin using stable isotopes. Mar. Chem. 221 https://doi.org/10.1016/j.marchem.2020.103756.

Morrison, R., Waldner, A., Hathorne, E.C., Rahlf, P., Zieringer, M., Montagna, P., Colin, C., Frank, N., Frank, M., 2019. Limited influence of basalt weathering inputs on the seawater neodymium isotope composition of the northern Iceland Basin. Chem. Geol. 511, 358–370. VSI. https://doi.org/10.1016/j.chemgeo.2018.10.019.

Nasemann, P., Janssen, D.J., Rickli, J., Grasse, P., Frank, M., Jaccard, S.L., 2020. Chromium reduction and associated stable isotope fractionation restricted to anoxic shelf waters in the Peruvian Oxygen Minimum Zone. Geochim. Cosmochim. Acta 285, 207–224. https://doi.org/10.1016/j.gca.2020.06.027.

Neuholz, R., Schnetger, B., Kleint, C., Koschinsky, A., Lettmann, K., Sander, S., Türke, A., Walter, M., Zitoun, R., Brumsack, H.J., 2020. Near-field hydrothermal plume dynamics at Brothers Volcano (Kermadec Arc): a short-lived radium isotope study. Chem. Geol. 533 https://doi.org/10.1016/j.chemgeo.2019.119379. VSI.

Nishioka, J., Obata, H., Ogawa, H., Ono, K., Yamashita, Y., Lee, K., Takeda, S., Yasuda, I., 2020. Subpolar marginal seas fuel the North Pacific through the intermediate water at the termination of the global ocean circulation. Proc. Natl. Acad. Sci. U. S. A. 117, 12665–12673. https://doi.org/10.1073/pnas.2000658117.

Ohnemus, D.C., Lam, P.J., 2015. Cycling of lithogenic marine particles in the US GEOTRACES North Atlantic transect. Deep Sea Res. II 116, 283–302. https://doi.org/10.1016/j.dsr2.2014.11.019.

Pahnke, K., van de Flierdt, T., Jones, K.M., Lambelet, M., Hemming, S.R., Goldstein, S.L., 2012. GEOTRACES intercalibration of neodymium isotopes and rare earth element concentrations in seawater and suspended particles. Part 2: systematic tests and baseline profiles. Limnol. Oceanogr. Methods 10, 252–269. https://doi.org/10.4319/lom.2012.10.252.

Paulukat, C., Døssing, L.N., Mondal, S.K., Voegelin, A.R., Frei, R., 2015. Oxidative release of chromium from Archean ultramafic rocks, its transport and environmental impact - A Cr isotope perspective on the Sukinda valley ore district (Orissa, India). Appl. Geochem. 59, 125–138. https://doi.org/10.1016/j.apgeochem.2015.04.016.

Paulukat, C., Gilleaudeau, G.J., Chernyavskiy, P., Frei, R., 2016. The Cr-isotope signature of surface seawater - a global perspective. Chem. Geol. 444, 101–109. https://doi.org/10.1016/j.chemgeo.2016.10.004.

Pereira, N.S., Voegelin, A.R., Paulukat, C., Sial, A.N., Ferreira, V.P., Frei, R., 2016. Chromium-isotope signatures in scleractinian corals from the Rocas Atoll, Tropical South Atlantic. Geobiology 14, 54–67. https://doi.org/10.1111/gbi.12155.

Pham, V.Q., Grenier, M., Cravatte, S., Michael, S., Jacquet, S., Belhadj, M., Nachez, Y., Germineaud, C., Jeandel, C., 2019. Dissolved rare earth elements distribution in the Solomon Sea. Chem. Geol. 524, 11–36. VSI. https://doi.org/10.1016/j.chemgeo.2019.05.012.

Piepgras, D.J., Wasserburg, G.J., Dasch, E.J., 1979. The isotopic composition of Nd in different ocean masses. Earth Planet. Sci. Lett. 45, 223–236. https://doi.org/10.1016/0012-821X(79)90125-0.

Posacka, A.M., Semeniuk, D.M., Whitby, H., van den Berg, C.M.G., Cullen, J.T., Orians, K., Maldonado, M.T., 2017. Dissolved copper (dCu) biogeochemical cycling in the subarctic Northeast Pacific and a call for improving methodologies. Mar. Chem. 196, 47–61. https://doi.org/10.1016/j.marchem.2017.05.007.

Prospero, J.M., Collard, F.X., Molinié, J., Jeannot, A., 2014. Characterizing the annual cycle of African dust transport to the Caribbean Basin and South America and its impact on the environment and air quality. Glob. Biogeochem. Cycles 28, 757–773. https://doi.org/10.1002/2013GB004802.

Radic, A., Lacan, F., Murray, J.W., 2011. Iron isotopes in the seawater of the equatorial Pacific Ocean: new constraints for the oceanic iron cycle. Earth Planet. Sci. Lett. 306, 1–10. https://doi.org/10.1016/j.epsl.2011.03.015.

Resing, J.A., Sedwick, P.N., German, C.R., Jenkins, W.J., Moffett, J.W., Sohst, B.M., Tagliabue, A., 2015. Basin-scale transport of hydrothermal dissolved metals across the South Pacific Ocean. Nature 523, 200–203. https://doi.org/10.1038/nature14577.

Revels, B.N., Ohnemus, D.C., Lam, P.J., Conway, T.M., John, S.G., 2015. The isotopic signature and distribution of particulate iron in the North Atlantic Ocean. Deep Sea Res. II 116, 321–331. https://doi.org/10.1016/j.dsr2.2014.12.004.

Rickli, J., Frank, M., Baker, A.R., Aciego, S., de Souza, G., Georg, R.B., Halliday, A.N., 2010. Hafnium and neodymium isotopes in surface waters of the eastern Atlantic Ocean: implications for sources and inputs of trace metals to the ocean. Geochim. Cosmochim. Acta 74, 540–557.

Rickli, J., Janssen, D.J., Hassler, C., Ellwood, M.J., Jaccard, S.L., 2019. Chromium biogeochemistry and stable isotope distribution in the Southern Ocean. Geochim. Cosmochim. Acta 262, 188–206. https://doi.org/10.1016/j.gca.2019.07.033.

Ripperger, S., Rehkämper, M., 2007. Precise determination of cadmium isotope fractionation in seawater by double spike MC-ICPMS. Geochim. Cosmochim. Acta 71, 631–642. https://doi.org/10.1016/j.gca.2006.10.005.

Ripperger, S., Rehkämper, M., Porcelli, D., Halliday, A.N., 2007. Cadmium isotope fractionation in seawater - a signature of biological activity. Earth Planet. Sci. Lett. 261, 670–684. https://doi.org/10.1016/j.epsl.2007.07.034.

Robinson, S., Ivanovic, R., van de Flierdt, T., Blanchet, C.L., Tachikawa, K., Martin, E.E., Cook, C.P., Williams, T., Gregoire, L., Plancherel, Y., Jeandel, C., Arsouze, T., 2021. Global continental and marine detrital εNd: an updated compilation for use in understanding marine Nd cycling. Chem. Geol. 567, 120119. https://doi.org/10.1016/j.chemgeo.2021.120119.

Rolison, J.M., Stirling, C.H., Middag, R., Gault-Ringold, M., George, E., Rijkenberg, M.J.A., 2018. Iron isotope fractionation during pyrite formation in a sulfidic Precambrian ocean analogue. Earth Planet. Sci. Lett. 488, 1–13. https://doi.org/10.1016/j.epsl.2018.02.006.

Roshan, S., Wu, J., 2018. Dissolved and colloidal copper in the tropical South Pacific. Geochim. Cosmochim. Acta 233, 81–94. https://doi.org/10.1016/j.gca.2018.05.008.

Rouxel, O.J., Auro, M.E., 2010. Iron isotope variations in coastal seawater determined by multicollector ICP-MS. Geostand. Geoanal. Res. 34, 135–144. https://doi.org/10.1111/j.1751-908X.2010.00063.x.

Roy-Barman, M., Pons-Branchu, E., Levier, M., Bordier, L., Foliot, L., Gdaniec, S., Ayrault, S., Garcia-Orellana, J., Masque, P., Castrillejo, M., 2019. Barium during the GEOTRACES GA-04S MedSeA cruise: the Mediterranean Sea Ba budget revisited. Chem. Geol. 511, 431–440. VSI. https://doi.org/10.1016/j.chemgeo.2018.09.015.

Samanta, M., Ellwood, M.J., Sinoir, M., Hassler, C.S., 2017. Dissolved zinc isotope cycling in the Tasman Sea, SW Pacific Ocean. Mar. Chem. 192, 1–12. https://doi.org/10.1016/j.marchem.2017.03.004.

Samanta, M., Ellwood, M.J., Strzepek, R.F., 2018. Zinc isotope fractionation by Emiliania huxleyi cultured across a range of free zinc ion concentrations. Limnol. Oceanogr. 63, 660–671. https://doi.org/10.1002/lno.10658.

Sanial, V., Kipp, L.E., Henderson, P.B., van Beek, P., Reyss, J.L., Hammond, D.E., Hawco, N.J., Saito, M.A., Resing, J.A., Sedwick, P., Moore, W.S., Charette, M.A., 2018. Radium-228 as a tracer of dissolved trace element inputs from the Peruvian continental margin. Mar. Chem. 201, 20–34. https://doi.org/10.1016/j.marchem.2017.05.008.

Santana-González, C., González-Dávila, M., Santana-Casiano, J.M., Gladyshev, S., Sokov, A., 2019. Organic matter effect on Fe(II) oxidation kinetics in the Labrador Sea. Chem. Geol. 511, 238–255. VSI. https://doi.org/10.1016/j.chemgeo.2018.12.019.

Sarmiento, J.L., Gruber, N., Brzezinski, M.A., Dunne, J.P., 2004. High-latitude controls of thermocline nutrients and low latitude biological productivity. Nature 427, 56–60. https://doi.org/10.1038/nature02127.

Sarmiento, J.L., Simeon, J., Gnanadesikan, A., Gruber, N., Key, R.M., Schlitzer, R., 2007. Deep ocean biogeochemistry of silicic acid and nitrate. Glob. Biogeochem. Cycles 21. https://doi.org/10.1029/2006GB002720.

Scheiderich, K., Amini, M., Holmden, C., Francois, R., 2015. Global variability of chromium isotopes in seawater demonstrated by Pacific, Atlantic, and Arctic Ocean samples. Earth Planet. Sci. Lett. 423, 87–97. https://doi.org/10.1016/j.epsl.2015.04.030.

Schlitzer, R., Anderson, R.F., Dodas, E.M., Lohan, M., Geibert, W., Tagliabue, A., Bowie, A., Jeandel, C., Maldonado, M.T., Landing, W.M., Cockwell, D., Abadie, C., Abouchami, W., Achterberg, E.P., Agather, A., Aguliar-Islas, A., van Aken, H.M., Andersen, M., Archer, C., Auro, M., de Baar, H.J., Baars, O., Baker, A.R., Bakker, K., Basak, C., Baskaran, M., Bates, N.R., Bauch, D., van Beek, P., Behrens, M.K., Black, E., Bluhm, K., Bopp, L., Bouman, H., Bowman, K., Bown, J., Boyd, P., Boye, M., Boyle, E.A., Branellec, P., Bridgestock, L., Brissebrat, G., Browning, T., Bruland, K.W., Brumsack, H.J., Brzezinski, M., Buck, C.S., Buck, K.N., Buesseler, K., Bull, A., Butler, E., Cai, P., Mor, P.C., Cardinal, D., Carlson, C., Carrasco, G., Casacuberta, N., Casciotti, K.L., Castrillejo, M., Chamizo, E., Chance, R., Charette, M.A., Chaves, J.E., Cheng, H., Chever, F., Christl, M., Church, T.M., Closset, I., Colman, A., Conway, T.M., Cossa, D., Croot, P., Cullen, J.T., Cutter, G.A., Daniels, C., Dehairs, F., Deng, F., Dieu, H.T., Duggan, B., Dulaquais, G., Dumousseaud, C., Echegoyen-Sanz, Y., Edwards, R.L., Ellwood, M., Fahrbach, E., Fitzsimmons, J.N., Russell Flegal, A., Fleisher, M.Q., van de Flierdt, T., Frank, M., Friedrich, J., Fripiat, F., Fröllje, H., Galer, S.J.G., Gamo, T., Ganeshram, R.S., Garcia-Orellana, J., Garcia-Solsona, E., Gault-Ringold, M., George, E., Gerringa, L.J.A., Gilbert, M., Godoy, J.M., Goldstein, S.L., Gonzalez, S.R., Grissom, K., Hammerschmidt, C., Hartman, A., Hassler, C.S., Hathorne, E.C., Hatta, M., Hawco, N., Hayes, C.T., Heimbürger, L.E., Helgoe, J., Heller, M., Henderson, G.M., Henderson, P.B., van Heuven, S., Ho, P., Horner, T.J., te Hsieh, Y., Huang, K.F., Humphreys, M.P., Isshiki, K., Jacquot, J.E., Janssen, D.J., Jenkins, W.J., John, S., Jones, E.M., Jones, J.L., Kadko, D.C., Kayser, R., Kenna, T.C., Khondoker, R., Kim, T., Kipp, L., Klar, J.K., Klunder, M., Kretschmer, S., Kumamoto, Y., Laan, P., Labatut, M., Lacan, F., Lam, P.J., Lambelet, M., Lamborg, C.H., le Moigne, F.A.C., le Roy, E., Lechtenfeld, O.J., Lee, J.M., Lherminier, P., Little, S., López-Lora, M., Lu, Y., Masque, P., Mawji, E., Mcclain, C.R., Measures, C., Mehic, S., Barraqueta, J.L.M., van der Merwe, P., Middag, R., Mieruch, S., Milne, A., Minami, T., Moffett, J.W., Moncoiffe, G., Moore, W.S., Morris, P.J., Morton, P.L., Nakaguchi, Y., Nakayama, N., Niedermiller, J., Nishioka, J., Nishiuchi, A., Noble, A., Obata, H., Ober, S., Ohnemus, D.C., van Ooijen, J., O'Sullivan, J., Owens, S., Pahnke, K., Paul, M., Pavia, F., Pena, L.D., Peters, B., Planchon, F., Planquette, H., Pradoux, C., Puigcorbé, V., Quay, P., Queroue, F., Radic, A., Rauschenberg, S., Rehkämper, M., Rember, R., Remenyi, T., Resing, J.A., Rickli, J., Rigaud, S., Rijkenberg, M.J.A., Rintoul, S., Robinson, L.F., Roca-Martí, M., Rodellas, V., Roeske, T., Rolison, J.M., Rosenberg, M., Roshan, S., Rutgers van der Loeff, M.M., Ryabenko, E., Saito, M.A., Salt, L.A., Sanial, V., Sarthou, G., Schallenberg, C., Schauer, U., Scher, H., Schlosser, C., Schnetger, B., Scott, P., Sedwick, P.N., Semiletov, I., Shelley, R., Sherrell, R.M., Shiller, A.M., Sigman, D.M., Singh, S.K., Slagter, H.A., Slater, E., Smethie, W.M., Snaith, H., Sohrin, Y., Sohst, B., Sonke, J.E., Speich, S., Steinfeldt, R., Stewart, G., Stichel, T., Stirling, C.H., Stutsman, J., Swarr, G.J., Swift, J.H., Thomas, A., Thorne, K., Till, C.P., Till, R., Townsend, A.T., Townsend, E., Tuerena, R., Twining, B.S., Vance, D., Velazquez, S., Venchiarutti, C., Villa-Alfageme, M., Vivancos, S.M., Voelker, A.H.L., Wake, B., Warner, M.J., Watson, R., van Weerlee, E., Alexandra Weigand, M., Weinstein, Y., Weiss, D., Wisotzki, A.,

Woodward, E.M.S., Wu, J., Wu, Y., Wuttig, K., Wyatt, N., Xiang, Y., Xie, R.C., Xue, Z., Yoshikawa, H., Zhang, J., Zhang, P., Zhao, Y., Zheng, L., Zheng, X.Y., Zieringer, M., Zimmer, L.A., Ziveri, P., Zunino, P., Zurbrick, C., 2018. The GEOTRACES intermediate data product 2017. Chem. Geol. 493, 210–223. VSI. https://doi.org/10.1016/j.chemgeo.2018.05.040.

SCOR Working Group, 2007. GEOTRACES – an international study of the global marine biogeochemical cycles of trace elements and their isotopes. Chem. Erde Geochem. 67, 85–131. https://doi.org/10.1016/j.chemer.2007.02.001.

Shelley, R.U., Morton, P., Landing, W.M., 2015. Elemental ratios and enrichment factors in aerosols from the US-GEOTRACES North Atlantic transects. Deep Sea Res. II 116, 262–272. https://doi.org/10.1016/j.dsr2.2014.12.005.

Shelley, R.U., Roca-Martí, M., Castrillejo, M., Sanial, V., Masqué, P., Landing, W.M., Planquette, H., Sarthou, G., 2017. Quantification of trace element atmospheric deposition fluxes to the Atlantic Ocean (>40°N; GEOVIDE, GEOTRACES GA01) during spring 2014. Deep. Res. I 119, 34–49. https://doi.org/10.1016/j.dsr.2016.11.010.

Siddall, M., Khatiwala, S., van de Flierdt, T., Jones, K., Goldstein, S.L., Hemming, S., Anderson, R.F., 2008. Towards explaining the Nd paradox using reversible scavenging in an ocean general circulation model. Earth Planet. Sci. Lett. 274 (3–4), 448–461. https://doi.org/10.1016/j.epsl.2008.07.044.

Sieber, M., Conway, T.M., de Souza, G.F., Obata, H., Takano, S., Sohrin, Y., Vance, D., 2019a. Physical and biogeochemical controls on the distribution of dissolved cadmium and its isotopes in the Southwest Pacific Ocean. Chem. Geol. 511, 494–509. VSI. https://doi.org/10.1016/j.chemgeo.2018.07.021.

Sieber, M., Conway, T.M., de Souza, G.F., Hassler, C.S., Ellwood, M., Vance, D., 2019b. High-resolution Cd isotope systematics in multiple zones of the Southern Ocean from the Antarctic Circumnavigation Expedition. Earth Planet. Sci. Lett. 527, 115799.

Sieber, M., Conway, T.M., de Souza, G.F., Hassler, C.S., Ellwood, M.J., Vance, D., 2020. Cycling of zinc and its isotopes across multiple zones of the Southern Ocean: insights from the Antarctic Circumnavigation Expedition. Geochim. Cosmochim. Acta 268, 310–324. https://doi.org/10.1016/j.gca.2019.09.039.

Sohrin, Y., Urushihara, S., Nakatsuka, S., Kono, T., Higo, E., Minami, T., Norisuye, K., Umetani, S., 2008. Multielemental determination of GEOTRACES key trace metals in seawater by ICPMS after preconcentration using an ethylenediaminetriacetic acid chelating resin. Anal. Chem. 80, 6267–6273. https://doi.org/10.1021/ac800500f.

Staubwasser, M., Schoenberg, R., von Blanckenburg, F., Krüger, S., Pohl, C., 2013. Isotope fractionation between dissolved and suspended particulate Fe in the oxic and anoxic water column of the Baltic Sea. Biogeosciences 10, 233–245. https://doi.org/10.5194/bg-10-233-2013.

Stichel, T., Hartman, A.E., Duggan, B., Goldstein, S.L., Scher, H., Pahnke, K., 2015. Separating biogeochemical cycling of neodymium from water mass mixing in the Eastern North Atlantic. Earth Planet. Sci. Lett. 412, 245–260. https://doi.org/10.1016/j.epsl.2014.12.008.

Stichel, T., Kretschmer, S., Geibert, W., Lambelet, M., Plancherel, Y., Rutgers van der Loeff, M., van de Flierdt, T., 2020. Particle-seawater Interaction of Neodymium in the North Atlantic, 4(9), pp. 1700–1717.

Tagliabue, A., Sallée, J.-B., Bowie, A.R., Lévy, M., Swart, S., Boyd, P.W., 2014. Surface-water iron supplies in the Southern Ocean sustained by deep winter mixing. Nat. Geosci. 7, 314–320. https://doi.org/10.1038/ngeo2101.

Takano, S., Tanimizu, M., Hirata, T., Sohrin, Y., 2013. Determination of isotopic composition of dissolved copper in seawater by multi-collector inductively coupled plasma mass spectrometry after pre-concentration using an ethylenediaminetriacetic acid chelating resin. Anal. Chim. Acta 784, 33–41. https://doi.org/10.1016/j.aca.2013.04.032.

Takano, S., Tanimizu, M., Hirata, T., Sohrin, 2014. Isotopic constraints on biogeochemical cycling of copper in the ocean. Nat. Commun. 5, 5663. https://doi.org/10.1038/ncomms6663.

Takano, S., Tanimizu, M., Hirata, T., Shin, K.-C.C., Fukami, Y., Suzuki, K., Sohrin, Y., 2017. A simple and rapid method for isotopic analysis of nickel, copper, and zinc in seawater using chelating extraction and anion exchange. Anal. Chim. Acta 967, 1–11. https://doi.org/10.1016/j.aca.2017.03.010.

Thompson, C.M., Ellwood, M.J., 2014. Dissolved copper isotope biogeochemistry in the Tasman Sea, SW Pacific Ocean. Mar. Chem. 165, 1–9. https://doi.org/10.1016/j.marchem.2014.06.009.

Thompson, C.M., Ellwood, M.J., Wille, M., 2013. A solvent extraction technique for the isotopic measurement of dissolved copper in seawater. Anal. Chim. Acta 775, 106–113. https://doi.org/10.1016/j.aca.2013.03.020.

Twining, B.S., Baines, S.B., 2013. The trace metal composition of marine phytoplankton. Annu. Rev. Mar. Sci. 5, 191–215. https://doi.org/10.1146/annurev-marine-121211-172322.

Urban, E.R., Bowie, A.R., Boyd, P.W., Buck, K.N., Lohan, M.C., Sander, S.G., Schlitzer, R., Tagliabue, A., Turner, D., 2020. The Importance of Bottom-up Approaches to International Cooperation in Ocean Science, 33, pp. 11–15. https://doi.org/10.2307/26897830.

van de Flierdt, T., Pahnke, K., Amakawa, H., Andersson, P., Basak, C., Coles, B., Colin, C., Crocket, K., Frank, M., Frank, N., Goldstein, S.L., Goswami, V., Haley, B.A., Hathorne, E.C., Hemming, S.R., Henderson, G.M., Jeandel, C., Jones, K., Kreissig, K., Lacan, F., Lambelet, M., Martin, E.E., Newkirk, D.R., Obata, H., Pena, L., Piotrowski, A.M., Pradoux, C., Scher, H.D., Schöberg, H., Singh, S.K., Stiche, T., Tazoe, H., Vance, D., Yang, J., 2012. GEOTRACES intercalibration of neodymium isotopes and rare earth element concentrations in seawater and suspended particles. Part 1: reproducibility of results for the international intercomparison. Limnol. Oceanogr. Methods 10, 234–251. https://doi.org/10.4319/lom.2012.10.234.

van de Flierdt, T., Grifths, A.M., Lambelet, M., Little, S.H., Stichel, T., Wilson, D.J., 2016. Neodymium in the oceans: a global database, a regional comparison and implications for palaeoceanographic research. Phil. Trans. R. Soc. A 374. https://doi.org/10.1098/rsta.2015.0293, 20150293, 20150293.

Vance, D., Archer, C., Bermin, J., Perkins, J., Statham, P.J., Lohan, M.C., Ellwood, M.J., Mills, R.A., 2008. The copper isotope geochemistry of rivers and the oceans. Earth Planet. Sci. Lett. 274, 204–213. https://doi.org/10.1016/j.epsl.2008.07.026.

Vance, D., Little, S.H., Archer, C., Cameron, V., Andersen, M.B., Rijkenberg, M.J.A., Lyons, T.W., 2016. The oceanic budgets of nickel and zinc isotopes: the importance of sulfidic environments as illustrated by the Black Sea. Philos. Trans. R. Soc. Lond. A 374, 37420150294.

Vance, D., Little, S.H., de Souza, G.F., Khatiwala, S., Lohan, M.C., Middag, R., 2017. Silicon and zinc biogeochemical cycles coupled through the Southern Ocean. Nat. Geosci. 10, 202–206. https://doi.org/10.1038/ngeo2890.

Vance, D., de Souza, G.F., Zhao, Y., Cullen, J.T., Lohan, M.C., 2019. The relationship between zinc, its isotopes, and the major nutrients in the North-East Pacific. Earth Planet. Sci. Lett. 525, 115748. https://doi.org/10.1016/j.epsl.2019.115748.

Villa-Alfageme, M., Chamizo, E., Kenna, T.C., López-Lora, M., Casacuberta, N., Chang, C., Masqué, P., Christl, M., 2019. Distribution of 236U in the U.S. GEOTRACES Eastern Pacific Zonal Transect and its use as a water mass tracer. Chem. Geol. 517, 44–57. https://doi.org/10.1016/j.chemgeo.2019.04.003.

Wang, R.M., Archer, C., Bowie, A.R., Vance, D., 2019a. Zinc and nickel isotopes in seawater from the Indian Sector of the Southern Ocean: the impact of natural iron fertilization versus Southern Ocean hydrography and biogeochemistry. Chem. Geol. 12, 12–34 (VSI).

Wang, X., Glass, J.B., Reinhard, C.T., Planavsky, N.J., 2019b. Species-dependent chromium isotope fractionation across the Eastern Tropical North Pacific Oxygen Minimum Zone. Geochem. Geophys. Geosyst. 20, 2499–2514. https://doi.org/10.1029/2018GC007883.

Weber, T., John, S.G., Tagliabue, A., DeVries, T., 2018. Biological uptake and reversible scavenging of zinc in the global ocean. Science 361, 72–76. https://doi.org/10.1126/science.aap8532.

Wu, J., Dai, M., Xu, Y., Zheng, J., 2019. Plutonium in the western North Pacific: transport along the Kuroshio and implication for the impact of Fukushima Daiichi Nuclear Power Plant accident. Chem. Geol. 511, 256–264. VSI. https://doi.org/10.1016/j.chemgeo.2018.12.006.

Xie, R.C., Galer, S.J., Abouchami, W., Rijkenberg, M.J., de Jong, J.T.M., de Baar, H.J., Andreae, M.O., 2015. The cadmium-phosphate relationship in the western South Atlantic – the importance of mode and intermediate waters on the global systematics. Mar. Chem. 177, 110–123. https://doi.org/10.1016/j.marchem.2015.06.011.

Xie, R.C., Galer, S.J.G., Abouchami, W., Rijkenberg, M.J.A., de Baar, H.J.W., De Jong, J., Andreae, M.O., 2017. Non-Rayleigh control of upper-ocean Cd isotope fractionation in the western South Atlantic. In: Earth and Planetary Science Letters. Elsevier B.V. https://doi.org/10.1016/j.epsl.2017.04.024.

Xie, R.C., Galer, S.J.G., Abouchami, W., Frank, M., 2019a. Limited impact of eolian and riverine sources on the biogeochemical cycling of Cd in the tropical Atlantic. Chem. Geol. 511, 371–379. VSI. https://doi.org/10.1016/j.chemgeo.2018.10.018.

Xie, R.C., Rehkämper, M., Grasse, P., van de Flierdt, T., Frank, M., Xue, Z., 2019b. Isotopic evidence for complex biogeochemical cycling of Cd in the eastern tropical South Pacific. Earth Planet. Sci. Lett. 512, 134–146. https://doi.org/10.1016/j.epsl.2019.02.001.

Xue, Z.C., Rehkämper, M., Schönbächler, M., Statham, P.J., Coles, B.J., Schönbächler, M., Coles, B.J., 2012. A new methodology for precise cadmium isotope analyses of seawater. Anal. Bioanal. Chem. 402, 883–893. https://doi.org/10.1007/s00216-011-5487-0.

Xue, Z.C., Rehkämper, M., Horner, T.J., Abouchami, W., Middag, R., van de Flierdt, T., de Baar, H.J.W.W., van de Flierd, T., de Baar, H.J.W.W., 2013. Cadmium isotope variations in the Southern Ocean. Earth Planet. Sci. Lett. 382, 161–172. https://doi.org/10.1016/j.epsl.2013.09.014.

Yang, S.C., Lee, D.-C., Ho, T.-Y., 2012. The isotopic composition of Cadmium in the water column of the South China Sea. Geochim. Cosmochim. Acta 98, 66–77. https://doi.org/10.1016/j.gca.2012.09.022.

Yang, S.C., Lee, D.-C., Ho, T.-Y., Wen, L.-S., Yang, H.-H., 2014. The isotopic composition of dissolved cadmium in the water column of the West Philippine Sea. Front. Mar. Sci. 1 https://doi.org/10.3389/fmars.2014.00061.

Yang, S.C., Zhang, J., Sohrin, Y., Ho, T.Y., 2018. Cadmium cycling in the water column of the Kuroshio-Oyashio Extension region: insights from dissolved and particulate isotopic composition. Geochim. Cosmochim. Acta 233, 66–80. https://doi.org/10.1016/j.gca.2018.05.001.

Yang, S.C., Hawco, N.J., Pinedo-González, P., Bian, X., Huang, K.F., Zhang, R., John, S.G., 2020. A new purification method for Ni and Cu stable isotopes in seawater provides evidence for widespread Ni isotope fractionation by phytoplankton in the North Pacific. Chem. Geol. 547, 119662. https://doi.org/10.1016/j.chemgeo.2020.119662.

Zhang, R., Jensen, L.T., Fitzsimmons, J.N., Sherrell, R.M., John, S.G., 2019. Dissolved cadmium and cadmium stable isotopes in the western Arctic Ocean. Geochim. Cosmochim. Acta 258, 258–273. https://doi.org/10.1016/j.gca.2019.05.028.

Zhao, Y., Vance, D., Abouchami, W., de Baar, H.J.W., 2014. Biogeochemical cycling of zinc and its isotopes in the Southern Ocean. Geochim. Cosmochim. Acta 125, 653–672. https://doi.org/10.1016/j.gca.2013.07.045.

Zieringer, M., Frank, M., Stumpf, R., Hathorne, E.C., 2019. The distribution of neodymium isotopes and concentrations in the eastern tropical North Atlantic. Chem. Geol. 511, 265–278. VSI. https://doi.org/10.1016/j.chemgeo.2018.11.024.